



1 **Bias corrections of GOSAT SWIR XCO₂ and XCH₄ with
2 TCCON data and their evaluation using aircraft
3 measurement data**

4

5 **M. Inoue^{1,*}, I. Morino¹, O. Uchino¹, T. Nakatsuru¹, Y. Yoshida¹, T. Yokota¹, D.
6 Wunch², P. O. Wennberg², C. M. Roehl², D. W. T. Griffith³, V. A. Velazco³, N. M.
7 Deutscher^{3,4}, T. Warneke⁴, J. Notholt⁴, J. Robinson⁵, V. Sherlock^{5,**}, F. Hase⁶, T.
8 Blumenstock⁶, M. Rettinger⁷, R. Sussmann⁷, E. Kyrö⁸, R. Kivi⁸, K. Shiomi⁹, S.
9 Kawakami⁹, M. De Mazière¹⁰, S. G. Arnold¹¹, D. G. Feist¹¹, E. A. Barrow¹², J.
10 Barney¹², M. Dubey¹³, M. Schneider⁶, L. Iraci¹⁴, J. R. Podolske¹⁴, P. Hillyard^{14,15},
11 T. Machida¹, Y. Sawa¹⁶, K. Tsuboi¹⁶, H. Matsueda¹⁶, C. Sweeney¹⁷, P. P. Tans¹⁷,
12 A. E. Andrews¹⁷, S. C. Biraud¹⁸, Y. Fukuyama¹⁹, J. V. Pittman²⁰, E. A. Kort^{21,2,***},
13 and T. Tanaka^{1,9,****}**

14

15 [1]{National Institute for Environmental Studies (NIES), Tsukuba, Japan}

16 [2]{California Institute for Technology, Pasadena, CA, USA}

17 [3]{Centre for Atmospheric Chemistry, University of Wollongong, New South Wales,
18 Australia}

19 [4]{Institute of Environmental Physics, University of Bremen, Bremen, Germany}

20 [5]{National Institute of Water and Atmospheric Research, Lauder, New Zealand}

21 [6]{IMK-ASF, Karlsruhe Institute of Technology, Karlsruhe, Germany}

22 [7]{IMK-IFU, Karlsruhe Institute of Technology, Garmisch-Partenkirchen, Germany}

23 [8]{Arctic Research Centre, Finnish Meteorological Institute (FMI), Sodankylä, Finland}

24 [9]{Japan Aerospace Exploration Agency (JAXA), Tsukuba, Japan}

25 [10]{Belgium Institute for Space Aeronomy (IASB-BIRA), Brussels, Belgium}

26 [11]{Max Planck Institute for Biogeochemistry (MPI-BGC), Jena, Germany}

27 [12]{Ivy Tech Community College of Indiana, Indianapolis, IN, USA}



- 1 [13] {Los Alamos National Laboratory, Los Alamos, NM, USA}
- 2 [14] {NASA Ames Research Center, Moffett Field, CA, USA}
- 3 [15] {Bay Area Environmental Research Institute, Petaluma, CA, USA}
- 4 [16] {Meteorological Research Institute (MRI), Tsukuba, Japan}
- 5 [17] {National Oceanic and Atmospheric Administration (NOAA), Boulder, CO, USA}
- 6 [18] {Lawrence Berkeley National Laboratory (LBNL), Berkeley, CA, USA}
- 7 [19] {Japan Meteorological Agency, Tokyo, Japan}
- 8 [20] {Department of Earth and Planetary Sciences, Harvard University, Cambridge, MA,
9 USA}
- 10 [21] {Jet Propulsion Laboratory, Pasadena, CA, USA}
- 11
- 12 [*] {now at: Department of Biological Environment, Akita Prefectural University, Akita,
13 Japan}
- 14 [**] {now at: Laboratoire de Météorologie Dynamique, Palaiseau, France}
- 15 [***] {now at: Department of Atmospheric, Oceanic and Space Sciences, University of
16 Michigan, Ann Arbor, MI, USA}
- 17 [****] {now at: NASA Ames Research Center, Moffett Field, CA, USA}
- 18
- 19 Correspondence to: M. Inoue (makoto@akita-pu.ac.jp)
- 20
- 21 **Abstract**
- 22
- 23 We describe a method for removing systematic biases of column-averaged dry air mole
24 fractions of CO₂ (XCO₂) and CH₄ (XCH₄) derived from short-wavelength infrared (SWIR)
25 spectra of the Greenhouse gases Observing SATellite (GOSAT). We conduct correlation
26 analyses between the GOSAT biases and simultaneously-retrieved auxiliary parameters. We
27 use these correlations to bias correct the GOSAT data, removing these spurious correlations.



1 Data from Total Carbon Column Observing Network (TCCON) were used as reference values
2 for this regression analysis. To evaluate the effectiveness of this correction method, the
3 uncorrected/corrected GOSAT data were compared to independent XCO₂ and XCH₄ data
4 derived from aircraft measurements taken for the Comprehensive Observation Network for
5 TRace gases by AIrLiner (CONTRAIL) project, the National Oceanic and Atmospheric
6 Administration (NOAA), the U.S. Department of Energy (DOE), the National Institute for
7 Environmental Studies (NIES), the Japan Meteorological Agency (JMA), the HIAPER Pole-
8 to-Pole observations (HIPPO) program, and the GOSAT validation aircraft observation
9 campaign over Japan. These comparisons demonstrate that the empirically-derived bias
10 correction improves the agreement between GOSAT XCO₂/XCH₄ and the aircraft data.
11 Finally, we present latitudinal distributions and temporal variations of the derived GOSAT
12 biases.

13

14 **1 Introduction**

15 Atmospheric carbon dioxide (CO₂) and methane (CH₄) are crucially important anthropogenic
16 greenhouse gases that contribute to global warming and future climate change. The
17 Greenhouse gases Observing SATellite (GOSAT), launched in January 2009, is the world's
18 first satellite specialized for measuring the concentrations of atmospheric CO₂ and CH₄ from
19 space (Yokota et al., 2009). Column-averaged dry air mole fractions of CO₂ (XCO₂) and CH₄
20 (XCH₄) are retrieved from the Short-Wavelength InfraRed (SWIR) spectra of the Thermal
21 And Near-infrared Sensor for carbon Observation - Fourier Transform Spectrometer
22 (TANSO-FTS) onboard GOSAT. Validation of XCO₂ and XCH₄ derived from the GOSAT
23 TANSO-FTS has been conducted by using ground-based high-resolution Fourier Transform
24 Spectrometer (ground-based FTS) data and aircraft measurements (Morino et al., 2011; Saitoh
25 et al., 2012; Yoshida et al., 2013; Inoue et al., 2013, 2014; Gavrilov et al., 2014). The results
26 showed that the GOSAT SWIR XCO₂ measurements (Ver. 02.00) are biased -1–2 ppm ($\pm 1\text{--}3$
27 ppm) against the aircraft measurement data (Inoue et al., 2013), whereas GOSAT SWIR
28 XCH₄ measurements (Ver. 02.00) are biased positively by 2–7 ppb with a standard deviation
29 of about 15 ppb (Inoue et al., 2014).

30

31 The systematic biases of the GOSAT XCO₂ and XCH₄ retrievals are produced by many
32 factors including aerosol optical depth, thin cirrus clouds, and surface pressure retrieval error



1 (e.g., Uchino et al., 2012; Yoshida et al., 2013). These biases can lead to large errors in the
2 estimations of regional fluxes of CO₂ and CH₄ from inversion analyses (Takagi et al., 2011;
3 Maksyutov et al., 2013; Deng et al., 2014; Ishizawa et al., in preparation). Consequently,
4 several studies have described bias corrections of the satellite retrieval data by using multiple
5 linear regression (e.g., Wunch et al., 2011b; Guerlet et al., 2013; Schneising et al., 2013).
6 Wunch et al. (2011b) have attempted to correct spatially and temporally varying biases in the
7 Atmospheric CO₂ Observations from Space retrievals of the GOSAT (ACOS-GOSAT;
8 O'Dell et al., 2012; Crisp et al., 2012) data obtained over land using an empirical linear
9 regression model with which they correlated variabilities in XCO₂ retrievals with surface
10 albedo, the difference between the retrieved and a priori surface pressure, airmass, and the
11 oxygen A-band spectral radiance. They used the GOSAT data in the Southern Hemisphere as
12 the reference values for the linear regression and evaluated the bias correction against the
13 Total Carbon Column Observing Network (TCCON) data from the Northern Hemisphere.
14

15 In this study, we develop a method for correcting the systematic biases of the GOSAT XCO₂
16 and XCH₄ retrievals (Ver. 02.21) provided by the National Institute for Environmental
17 Studies (NIES-GOSAT; Yoshida et al., 2013). Our method has three primary differences from
18 Wunch et al. (2011b): (1) we explicitly use TCCON data from numerous sites throughout the
19 world as reference values for the regression analysis; (2) the regression variables and
20 coefficients for correction of GOSAT data are determined separately for observations made
21 over land and those made over the ocean; and (3) we perform this analysis for both XCO₂ and
22 XCH₄. Such a partitioning is sensible because in the SWIR XCO₂ and XCH₄ retrievals, the
23 handling of the surface reflectance is different over land and ocean. In addition, the
24 atmosphere over ocean is generally cleaner than that over land because of the absence of
25 polluted air and aerosols from urban areas. These differences suggest that the bias
26 characteristics of XCO₂ and XCH₄ retrieved over ocean differ from those over land.
27

28 This paper is structured as follows. Sect. 2 presents a brief note on the datasets used and
29 analysis procedure. In Sect. 3, we show a detailed method for correcting GOSAT data and the
30 results of the empirical correction. Our findings and conclusions are given in Sect. 4.

31



1 **2 Data and analysis methods**

2 **2.1 XCO₂ and XCH₄ retrieved from GOSAT TANSO-FTS SWIR spectra**

3

4 To monitor the spatial distribution of atmospheric greenhouse gases from space, GOSAT was
5 launched on 23 January 2009 into a sun-synchronous orbit with an overpass time of roughly
6 13:00 local time (Kuze et al., 2009). Over a three-day period, TANSO-FTS onboard GOSAT
7 makes observations above several tens of thousands of ground points spread over the earth's
8 surface. Measurements in the SWIR and thermal infrared (TIR) bands of TANSO-FTS allow
9 the retrievals over cloud-free regions of XCO₂ and XCH₄, and CO₂ and CH₄ profiles,
10 respectively. (Yoshida et al., 2011, 2013; Saitoh et al., 2012). In this study, we used Ver.
11 02.21 XCO₂ and XCH₄ data (Yoshida et al., 2013), which cover the period from April 2009 to
12 May 2014.

13

14 **2.2 TCCON data**

15 The Total Carbon Column Observing Network (TCCON) is a worldwide network of ground-
16 based FTSSs that provide time series of column-averaged abundances of various atmospheric
17 constituents. These constituents, which include CO₂ and CH₄, are retrieved from near-infrared
18 solar absorption spectra using a nonlinear least-squares fitting algorithm referred to as GFIT
19 (Wunch et al., 2010, 2011a). The TCCON data have been used to compare with satellite data
20 and model simulations (Dils et al., 2006; Morino et al., 2011; Schneising et al., 2012; Saito et
21 al., 2012; Heyman et al., 2012; Oshchepkov et al., 2013; Yoshida et al., 2013; Belikov et al.,
22 2013; Dils et al., 2014; Nguyen et al., 2014; Scheepmaker et al., 2015) and elucidate the
23 temporal behavior of greenhouse gases (Wunch et al., 2009; Deutscher et al., 2010, 2014;
24 Messerschmidt et al., 2010; Ishizawa et al., 2015). In this study, we used TCCON data
25 analyzed with the GGG2014 version of the standard TCCON retrieval algorithm (Wunch et
26 al., 2015) for correction of GOSAT data. The TCCON data are available from the Carbon
27 Dioxide Information Analysis Center (CDIAC) at <http://tccon.ornl.gov>. The distribution and
28 basic information of 23 TCCON sites used for correction or validation analyses of GOSAT
29 data are shown in Fig. 1a and Table 1, respectively. The TCCON sites are distributed
30 throughout the world including North America, Europe, Asia, and Oceania (Fig. 1a). Due to



1 the absence of coincidence with GOSAT data at Ny Ålesund, these TCCON XCO₂ and XCH₄
2 data were not used for correction of GOSAT data; they were, however, used for the analysis of
3 latitudinal distributions described in Sect. 3.3.

4

5 **2.3 Aircraft-based data**

6 In order to test for remaining biases in the GOSAT data after applying the empirical
7 correction developed using TCCON data, we use aircraft profile data provided by the
8 Comprehensive Observation Network for TRace gases by AIrLiner (CONTRAIL) project
9 (Machida et al., 2008), the NOAA Earth System Research Laboratory/Global Monitoring
10 Division (ESRL/GMD; Xiong et al., 2008; Sweeney et al., 2015), the U.S. Department of
11 Energy (DOE; Biraud et al., 2013; Schmid et al., 2014), the National Institute for
12 Environmental Studies (NIES; Machida et al., 2001), the Japan Meteorological Agency
13 (JMA; Tsuboi et al., 2013), the HIAPER Pole-to-Pole Observations (HIPPO) project (Wofsy
14 et al., 2011, 2012; Kort et al., 2012; Santoni et al., 2014), and an aircraft measurement
15 campaign by NIES and the Japan Aerospace Exploration Agency (JAXA) (Tanaka et al.,
16 2012). To calculate aircraft-based XCO₂ and XCH₄ (as described in the next paragraph), we
17 also used tower data from the Meteorological Research Institute (MRI) in Tsukuba (Inoue and
18 Matsueda, 1996, 2001) and the NOAA ESRL/GMD tall tower network in Park Falls, WI and
19 West Branch, IA (Andrews et al., 2014). Details of the aircraft and tower measurements are
20 described in Inoue et al. (2013) and Inoue et al. (2014), except for the JMA aircraft and
21 ground-based measurements. The JMA aircraft measurements are conducted by utilizing the
22 cargo aircraft C-130H of the Japan Ministry of Defense (MOD) to collect flask air samples
23 once a month during a regular flight between the mainland of Japan and Minamitorishima, an
24 island located nearly 2000 km southeast of Tokyo (Tsuboi et al., 2013). In addition, the JMA
25 routinely obtains ground-based measurements at a height of 20 m over Minamitorishima. We
26 used CO₂ and CH₄ profiles from around Minamitorishima derived from aircraft and ground-
27 based data available via the World Data Centre for Greenhouse Gases (WDCGG) website
28 (<http://ds.data.jma.go.jp/gmd/wdcgg/>). The typical JMA aircraft sampling altitudes were 0.5–
29 6.5 km. Figure 1b and Table 2 show a horizontal map and basic information, respectively, on
30 every aircraft measurement site used in this study.

31



1 Aircraft-based XCO₂ and XCH₄ are calculated by applying the GOSAT SWIR column
2 averaging kernels (CAK) by using the methods developed by Miyamoto et al. (2013) and
3 Inoue et al. (2014), respectively. There is one difference in the aircraft XCH₄ calculation:
4 Inoue et al. (2014) used fixed monthly climatologies for the CH₄ profiles above the
5 tropopause and did not include the yearly trend in CH₄ concentration because of their short
6 analysis period (June 2009 to July 2010). In this study, the yearly trend is explicitly taken into
7 account. According to recent reports from the World Meteorological Organization (WMO),
8 global CH₄ abundance increased from 1789 ppb in 2007 to a high of 1824 ppb in 2013 (WMO,
9 2008, 2014) with a growth rate of about 6 ppb yr⁻¹. Here, we included this mean annual trend
10 (6 ppb yr⁻¹) of CH₄ profiles above the tropopause for the calculation of aircraft-based XCH₄.

11

12 **2.4 Correction and validation procedure of GOSAT data**

13 Our aim in this study is to correct GOSAT SWIR XCO₂ and XCH₄ (Ver. 02.21) by multiple
14 linear regression using TCCON data as reference values. In Sect. 3.1, we explain the details
15 of the empirical correction method. To evaluate the effectiveness of this correction method,
16 we compare uncorrected/corrected GOSAT XCO₂ (XCH₄) to independent aircraft-based
17 XCO₂ (XCH₄) based on aircraft measurements by CONTRAIL, NOAA, DOE, NIES, JMA,
18 the HIPPO project, and the NIES-JAXA joint campaign (Sect. 3.2). We compare GOSAT
19 data retrieved on the same day and within $\pm 5^\circ$ latitude/longitude boxes centered on each
20 aircraft profile. We also investigate the spatial distributions of uncorrected/corrected GOSAT
21 data (Sect. 3.3), and the temporal behavior of the GOSAT XCO₂ and XCH₄ biases (Sect. 3.4).

22

23 **3 Results and discussion**

24 **3.1 Parameter dependency of GOSAT biases and multiple linear regression 25 for correction of GOSAT data**

26 The bias correction of GOSAT XCO₂ and XCH₄ (Ver. 02.21) uses multiple linear regression.
27 Before formulating the regression equations, we perform a correlation analysis between the
28 GOSAT biases and simultaneously-retrieved auxiliary parameters at TCCON sites. Here, the
29 differences between GOSAT XCO₂ (XCH₄) and TCCON XCO₂ (XCH₄) are referred to as
30 Δ XCO₂ (Δ XCH₄). Figures 2a–d and 3a show several examples of scatter diagrams between



1 ΔXCO_2 (or ΔXCH_4) and simultaneously-retrieved auxiliary parameters obtained within $\pm 5^\circ$
2 latitude/longitude boxes centered at respective TCCON sites. The GOSAT data retrieved over
3 land and ocean regions are described by green and blue dots, respectively. For instance,
4 ΔXCO_2 has a significant negative correlation with the difference between the retrieved
5 surface pressure and a priori surface pressure (ΔP_s ; Fig. 2b), which suggests that error in the
6 surface pressure retrieval (ΔP_s) is, in part, responsible for the presence of the GOSAT XCO₂
7 biases. Thus, we examined the correlations between the GOSAT biases and more than 20
8 other parameters retrieved from GOSAT TANSO-FTS, and investigated which combinations
9 of available parameters led to a reduction of the GOSAT biases due to the linear regression.
10 For the correction of XCO₂ retrievals, we selected four parameters to include in bias
11 corrections; the retrieved aerosol optical depth (AOD), ΔP_s , airmass, and surface albedo for
12 the O₂ A-band. The derived bias correction for XCO₂ is

$$13 \quad X_{CO_2}^{modified} = X_{CO_2}^{retrieved} + C_0 - C_1(AOD - \overline{AOD}) - C_2(\Delta P_s - \overline{\Delta P_s}) \\ - C_3(airmass - \overline{airmass}) - C_4(albedo_O_2 - \overline{albedo_O_2}). \quad (1)$$

14 However, only the retrieved AOD was selected for XCH₄ retrievals. The bias correction for
15 XCH₄ is

$$16 \quad X_{CH_4}^{modified} = X_{CH_4}^{retrieved} + C_0 - C_1(AOD - \overline{AOD}). \quad (2)$$

17 Here, $X_{CO_2}^{retrieved}$ and $X_{CH_4}^{retrieved}$ are the GOSAT XCO₂ and XCH₄ retrievals, respectively (i.e.,
18 uncorrected GOSAT data). $X_{CO_2}^{modified}$ and $X_{CH_4}^{modified}$ denote the corrected GOSAT XCO₂ and
19 XCH₄ data, respectively. AOD represents the retrieved aerosol optical depth, and ΔP_s is the
20 difference between the retrieved surface pressure and the a priori surface pressure. Airmass is
21 a simple function of the solar zenith angle θ_z and the satellite-viewing angle θ_v and can be
22 approximated as

$$23 \quad airmass = \frac{1}{\cos \theta_z} + \frac{1}{\cos \theta_v}. \quad (3)$$

24 In addition, albedo_O₂ is the surface albedo for the O₂ A-band, which is retrieved only for
25 land. The overbars denote averages of all GOSAT data used for the regression analysis. C₀ is
26 the regression coefficient for the bias, and C₁, C₂, C₃, and C₄ are the regression coefficients
27 for the respective parameters, that are used for the correction of GOSAT data. As described in



1 the next paragraph, we determined these regression coefficients separately for land and ocean
2 regions.

3

4 Table 3 shows the regression coefficients obtained via the multiple linear regression analyses.
5 The coefficients, C₀–C₄, were determined as follows: To prepare the TCCON XCO₂ and
6 XCH₄ as reference values for the multiple regression analysis, we made a connection between
7 the GOSAT data retrieved within ±5° latitude/longitude boxes centered at respective TCCON
8 sites and mean values of TCCON data (GGG2014 version) observed within ±30 min of the
9 GOSAT overpass time. Averages and the standard deviations (SD) of the differences between
10 uncorrected GOSAT data and TCCON data at each site are listed in Table 4 for XCO₂ and
11 Table 5 for XCH₄. Figures 4a and 4c are scatter diagrams between uncorrected GOSAT data
12 and TCCON data at all TCCON sites for XCO₂ and XCH₄, respectively. For XCO₂, we
13 identify 8245 samples for land and 544 samples for ocean that satisfy the coincident criteria.
14 We find that global mean biases of GOSAT XCO₂ retrievals (i.e., uncorrected GOSAT
15 XCO₂) over land and ocean regions against the TCCON data were -0.86 ppm (SD = 2.18
16 ppm) and -1.90 ppm (SD = 1.72 ppm), respectively (Table 4). The average and standard
17 deviation of the GOSAT biases derived from respective TCCON sites (hereafter referred to as
18 station bias) over land are -0.43 ppm and 0.87 ppm, respectively. Correlation coefficients
19 between two XCO₂ datasets were 0.89 over land and 0.90 over ocean (Fig. 4a). The mean
20 biases of uncorrected GOSAT XCH₄ over land and ocean regions were -6.0 ppb (SD = 15.2
21 ppb) and -0.2 ppb (SD = 13.4 ppb), respectively (Table 5). Correlation coefficients between
22 both XCH₄ datasets were 0.85 over land and 0.91 over ocean (Fig. 4c). The results over land
23 are similar to those of Yoshida et al. (2013) who validated GOSAT XCO₂ and XCH₄ data
24 (Ver. 02.xx), although the versions of the TCCON data used in their study (the previous
25 GGG2012 version) and our present study differ. Conducting the regression analysis using Eqs.
26 (1) and (2), the regression coefficients for correction of GOSAT XCO₂ (and XCH₄) were
27 determined separately for land and ocean regions (Table 3). Because surface albedo is not
28 retrieved over ocean, the terms including C₄ in Eq. (1) were neglected for determining the
29 regression coefficients for XCO₂ over ocean. The GOSAT data were obtained through two
30 different TANSO-FTS modes: medium gain (Gain-M) utilized over bright land surfaces
31 including the Sahara Desert and high gain (Gain-H) used elsewhere (Yoshida et al., 2013).
32 Note that the regression coefficients are calculated from GOSAT data retrieved within ±5°



1 boxes centered at 20 TCCON sites, that are located in Gain-H regions even though we aim to
2 correct GOSAT XCO₂ and XCH₄ data from around the world, including Gain-H and Gain-M
3 regions. Additionally, we take the mean difference between TCCON XCH₄ and aircraft-based
4 XCH₄ into account when calculating the coefficients C₀ over land and ocean for XCH₄. In a
5 comparative analysis at four locations, Inoue et al. (2014) showed that aircraft-based XCH₄
6 was 8.6 ppb smaller than TCCON XCH₄ on average. Consequently, in this study, we used the
7 values for C₀ shown in Table 3b (i.e., 6.0 ppb over land and 0.2 ppb over ocean) for the
8 correction of GOSAT XCH₄ when comparing GOSAT XCH₄ with TCCON XCH₄. In contrast,
9 the values for C₀ shown in Table 3b with 8.6 ppb subtracted (i.e., -2.6 ppb over land and -8.4
10 ppb over ocean) were used when comparing the GOSAT XCH₄ with the aircraft-based XCH₄.
11 Figures 2e–h and 3b are scatter diagrams between the biases of GOSAT data (Δ XCO₂ and
12 Δ XCH₄) corrected by these regression coefficients C₀–C₄ (Table 3) and simultaneously
13 retrieved parameters. After correction, the correlation coefficients between Δ XCO₂ (or
14 Δ XCH₄) and respective parameters were approximately zero.

15

16 We compare the GOSAT XCO₂ and XCH₄ corrected using the regression coefficients to the
17 TCCON XCO₂ and XCH₄ (Tables 4–5, and Figs. 4b and 4d). Using this empirical correction,
18 the global mean biases of GOSAT XCO₂ relative to the TCCON data became zero over both
19 land (change from -0.86 ppm to 0.00 ppm) and ocean (-1.90 ppm to -0.01 ppm). Correlation
20 coefficients between GOSAT XCO₂ and TCCON XCO₂ became somewhat higher over land
21 (0.89 to 0.91). Table 5 shows that the mean biases of GOSAT XCH₄ also became zero over
22 both land (-6.0 ppb to 0.0 ppb) and ocean (-0.2 ppb to -0.1 ppb). Clearly, as expected, the
23 GOSAT XCO₂ and XCH₄ biases were reduced after correction. This, of course, is a natural
24 consequence because the GOSAT data approached the TCCON values after applying the
25 corrections. Therefore, in the next section, we validate the GOSAT XCO₂ and XCH₄
26 corrected by TCCON data using independent aircraft measurement data instead of TCCON
27 data.

28



1 **3.2 Comparisons between uncorrected/corrected GOSAT data and aircraft-based data**

2 To confirm the effectiveness of the empirical correction, we compare uncorrected/corrected
3 GOSAT data with aircraft-based data. Figure 5 shows scatter diagrams between
4 uncorrected/corrected GOSAT data and aircraft-based data at all aircraft observation sites.
5 Tables 6 and 7 indicate the differences between uncorrected/corrected GOSAT data and
6 aircraft-based data for XCO₂ and XCH₄ at each aircraft site, respectively. The average
7 differences between uncorrected GOSAT XCO₂ and aircraft-based XCO₂ over land and ocean
8 within $\pm 5^\circ$ latitude/longitude boxes were -0.85 ppm (SD = 2.48 ppm) and -2.08 ppm (SD =
9 1.69 ppm), respectively (Table 6). The correction reduced the mean biases of GOSAT XCO₂
10 to below twentieth over land (-0.85 ppm to -0.04 ppm) and to below one-sixth over ocean (-
11 2.08 ppm to -0.32 ppm). The averages of the XCO₂ station bias over land and ocean are also
12 smaller after correction. The correlation coefficients between GOSAT XCO₂ and aircraft-
13 based XCO₂ over land became higher after correction (0.86 to 0.88). For XCH₄, the average
14 differences between uncorrected GOSAT XCH₄ and aircraft-based XCH₄ over land and ocean
15 were 4.5 ppb (SD = 15.2 ppb) and 6.6 ppb (SD = 12.8 ppb), respectively (Table 7). The global
16 mean biases of GOSAT XCH₄ relative to aircraft measurements were also reduced by half
17 over land (4.5 ppb to 2.2 ppb) and reduced to about one-quarter over ocean (6.6 ppb to -1.7
18 ppb). The correlation coefficients between GOSAT XCH₄ and aircraft-based XCH₄ over land
19 became higher (0.70 to 0.71). Thus, the bias correction improves the accuracy and precision
20 of the GOSAT data for both XCO₂ and XCH₄.

22

23 **3.3 Spatial distributions of uncorrected/corrected GOSAT data**

24 We next applied the regression coefficients C₀–C₄ calculated from samples around only 20
25 TCCON sites to all GOSAT XCO₂ and XCH₄ data around the world, and we examined how
26 the global distributions of GOSAT data changed due to this empirical correction. Figures 6a
27 and 6b indicate the horizontal distributions of uncorrected GOSAT XCO₂ and corrected
28 GOSAT XCO₂, respectively, in July 2009. In the Northern summer, the CO₂ concentration
29 over Siberia is significantly lower due to forest absorption of CO₂ through photosynthesis
30 (e.g., Nakazawa et al., 1997; Guerlet et al., 2013). The differences between corrected GOSAT
31 XCO₂ and uncorrected GOSAT XCO₂ are shown in Fig. 6c. As noted above, GOSAT XCO₂



1 has a negative bias of about 1–2 ppm over land and ocean regions. Therefore, the bias
2 correction increases XCO₂ in most parts of the world (Fig. 6c). In the middle of South
3 America and southern Africa, however, GOSAT XCO₂ became smaller after correction. We
4 next focus on the horizontal distributions of uncorrected/corrected GOSAT XCH₄ in July
5 2009 (Figs. 6d and 6e). Figure 6d shows that CH₄ concentrations in the Northern Hemisphere
6 are higher than those in the Southern Hemisphere. In particular, there are distinct features of
7 high CH₄ concentrations around the eastern United States, the Middle East, western Siberia,
8 and East Asia in the Northern Hemisphere and low CH₄ concentrations over southern South
9 America, southern Africa, and Australia, with a larger gradient in the Southern Hemisphere.
10 After correction, GOSAT XCH₄ became 4–8 ppb higher over most land regions (Fig. 6f),
11 consistent with comparisons to the TCCON data over land (Sect. 3.1). XCH₄ over the ocean
12 became smaller at low latitudes in the Northern Hemisphere (0°–20°N) such as the Atlantic
13 Ocean, and became larger in mid-latitudes (20°–40°N).

14

15 It is difficult to evaluate whether the GOSAT data across the globe are improved by using the
16 regression coefficients C₀–C₄ derived exclusively from around TCCON sites, due to the
17 sparseness of the ground-based and aircraft measurements in many regions around the world.
18 Accordingly, we investigated the latitudinal distributions of the uncorrected/corrected
19 GOSAT data, the TCCON data, and the aircraft-based data, and then compared the three
20 datasets for July 2009 (Fig. 7). We prepared zonal-mean monthly averages of the GOSAT
21 data retrieved in each 15° latitudinal band. For example, averages of GOSAT XCO₂ obtained
22 over land and ocean regions within a latitudinal band from the equator to 15°N in July 2009
23 are represented by black and green dots, respectively, around 7.5°N in Fig. 7a. The TCCON
24 data are mean values measured within ±30 min of the GOSAT overpass time (e.g., about
25 12:50 pm local time in Tsukuba) on all days when TCCON data were obtained in July 2009.
26 Aircraft-based data are monthly averages of all data obtained at each aircraft observation site.
27 In July 2009, GOSAT XCO₂ data were underestimated by about 1–2 ppm compared to the
28 reference data (Fig. 7a). We found that corrected GOSAT XCO₂ was consistent with the
29 TCCON XCO₂ and aircraft-based XCO₂ in both hemispheres, though the variability of
30 aircraft-based XCO₂ was relatively large in mid-latitudes (Fig. 7b). Figure 7c shows
31 latitudinal distributions of uncorrected GOSAT XCH₄, TCCON XCH₄, and aircraft-based
32 XCH₄. XCH₄ in the Northern Hemisphere is higher than that in the Southern Hemisphere in



1 July (Fig. 7c), because the main CH₄ sources are terrestrial, including rice paddy fields and
2 wetlands. In addition, the latitudinal variation in XCH₄ shows a larger meridional gradient in
3 the Southern Hemisphere (Fig. 7c), which is consistent with the global distribution of XCH₄
4 (Fig. 6d). The uncorrected GOSAT XCH₄ was negatively biased against the TCCON data.
5 The empirical correction resulted in a marked decrease in GOSAT XCH₄ biases on the same
6 latitudinal bands as several TCCON sites (e.g., Ny Ålesund, Sodankylä, and Lauder) over both
7 hemispheres (Fig. 7d). Thus, the correction method is very effective for reducing the biases of
8 the GOSAT XCO₂ and XCH₄, from the standpoint of the spatial distributions.

9

10 **3.4 Temporal behaviors of uncorrected/corrected GOSAT data and the
11 GOSAT biases**

12 Finally, we investigated temporal variations in GOSAT XCO₂ and XCH₄ data and the
13 GOSAT biases. We focused on the 30°–45°N latitudinal band, which includes the Lamont site
14 where most monthly data were available during the analysis period. Figure 8a shows the
15 temporal variations of uncorrected GOSAT XCO₂, TCCON XCO₂ at Tsukuba and Lamont,
16 and aircraft-based XCO₂ at Narita. Along with the example of July 2009 in Sect. 3.3, zonal-
17 mean GOSAT XCO₂ retrieved over land and ocean regions within a 30°–45°N latitudinal
18 band, TCCON XCO₂ and aircraft-based XCO₂ at several sites included in a 30°–45°N
19 latitudinal band were calculated for all months during the analysis period. The temporal
20 variations in the three datasets revealed that XCO₂ is higher in Northern spring (April and
21 May) and lower in August and September (Fig. 8a). XCO₂ has a seasonal amplitude of
22 approximately 7–12 ppm at mid-latitudes over the Northern Hemisphere. In this study, the
23 growth rate of uncorrected GOSAT XCO₂ was roughly 2.5 ppm yr⁻¹ from 2009 to 2013,
24 while Inoue et al. (2013) showed that the growth rate of aircraft-based XCO₂ at most sites was
25 about 2.0 ppm yr⁻¹ from 2007 to 2010. This is consistent with the rapid increase of CO₂
26 emissions over the last few years. After bias correction, the temporal variability in the
27 GOSAT XCO₂ agrees well with those of the TCCON and aircraft measurements (Fig. 8b).
28 Moreover, the uncorrected GOSAT XCO₂ data were negatively biased (Fig. 8c), however,
29 this time series has a seasonality wherein the negative biases of GOSAT XCO₂ become higher
30 around July and August. After bias correction, the XCO₂ biases for many months approach
31 zero, though the seasonality in the difference remains (Fig. 8d).



1

2 Figure 9a shows the temporal behavior of zonal-mean uncorrected GOSAT XCH₄ and XCH₄
3 at the Tsukuba and Lamont TCCON sites. GOSAT XCH₄ is higher in September and October,
4 and lower in February and March than the reference data. Although the GOSAT XCH₄ data
5 retrieved over land were negatively biased except for summer during the analysis period (Figs.
6 9a and 9c), the GOSAT XCH₄ biases were reduced as a result of the empirical correction
7 (Figs. 9b and 9d). Consequently, we suggest that the bias correction method was effective for
8 GOSAT XCO₂ and XCH₄.

9

10 **4 Summary and conclusions**

11 In this study, we correct XCO₂ and XCH₄ data (Ver. 02.21) retrieved from the GOSAT
12 TANSO-FTS SWIR spectra. First, we conducted correlation analyses between the GOSAT
13 biases and the simultaneously-retrieved auxiliary parameters, using GOSAT data around
14 TCCON sites. Based on the results, we selected several parameters and determined the
15 regression coefficients for the correction of GOSAT XCO₂ and XCH₄ for land and ocean
16 regions separately. To evaluate the effectiveness of the bias correction method, the
17 uncorrected/corrected GOSAT XCO₂ and XCH₄ data were compared to aircraft
18 measurements provided by CONTRAIL, NOAA, DOE, NIES, JMA, the HIPPO project, and
19 the NIES-JAXA joint campaign. After correction, biases of GOSAT XCO₂ were reduced by a
20 factor of more than 20 over land and by a factor of six over ocean, while the biases of
21 GOSAT XCH₄ were reduced by half over land and became by almost a quarter of their
22 uncorrected values over ocean. We thus demonstrated that our empirical method using
23 multiple linear regression is useful for the bias correction of GOSAT XCO₂ and XCH₄.

24

25 **Acknowledgments**

26 The authors thank the many staff members of Japan Airlines, the JAL Foundation, and
27 JAMCO Tokyo for supporting the CONTRAIL project. We are grateful to the NOAA
28 ESRL/GMD tall tower network (K. Davis, A. Desai, R. Teclaw, D. Baumann, and C. Stanier)
29 for providing CO₂ tower data for Park Falls and West Branch. DOE flights were supported by
30 the Office of Biological and Environmental Research of the U.S. Department of Energy under
31 contract No. DE-AC02-05CH11231 as part of the Atmospheric Radiation Measurement



1 Program (ARM), ARM Aerial Facility, and Terrestrial Ecosystem Science Program. We
2 gratefully thank many staff members of the Japan Ministry of Defense for supporting the
3 JMA's ground-based and aircraft measurements. We also acknowledge the HIPPO team
4 members for CO₂ and CH₄ profile data from HIPPO missions. The HIPPO program is
5 supported by the National Science Foundation (NSF), and its operation is managed by the
6 Earth Observing Laboratory (EOL) of the National Center for Atmospheric Research (NCAR).
7 We also thank the Canadian Space Agency (CSA), which provides most of the funding
8 support for ACE. We are grateful to the HALOE team for publishing their data for scientific
9 use. This research was supported in part by the Environment Research and Technology
10 Development Fund (2A-1102) of the Ministry of the Environment, Japan. TCCON
11 measurements from Pasadena, Lamont, Park Falls and Darwin are funded by NASA grant
12 NNX14AI60G and NASA Orbiting Carbon Observatory Program. We are grateful to the
13 DOE ARM program for technical support of TCCON in Lamont and Darwin and to Jeff
14 Ayers for technical support of the TCCON measurements in Park Falls. Darwin and
15 Wollongong TCCON measurements are also supported by Australian Research Council grant
16 DP140101552 and Nicholas Deutscher is supported by an ARC-DECRA Fellowship,
17 DE140100178. The University of Bremen acknowledges the support of the EU projects
18 InGOS, and ICOS-INWIRE, and the Senate of Bremen for support of TCCON measurements
19 in Białystok, Bremen, Ny Ålesund, and Orléans. Operation of the Ascension Island site was
20 funded by the Max Planck Society. Research at the FMI was supported by the Academy of
21 Finland under grant number 140408.

22

23 **References**

24 Andrews, A. E., Kofler, J. D., Trudeau, M. E., Williams, J. C., Neff, D. H., Masarie, K. A.,
25 Chao, D. Y., Kitzis, D. R., Novelli, P. C., Zhao, C. L., Dlugokencky, E. J., Lang, P. M.,
26 Crotwell, M. J., Fischer, M. L., Parker, M. J., Lee, J. T., Baumann, D. D., Desai, A. R.,
27 Stanier, C. O., De Wekker, S. F. J., Wolfe, D. E., Munger, J. W., and Tans, P. P.: CO₂, CO,
28 and CH₄ measurements from tall towers in the NOAA Earth System Research Laboratory's
29 Global Greenhouse Gas Reference Network: instrumentation, uncertainty analysis, and
30 recommendations for future high-accuracy greenhouse gas monitoring efforts, *Atmos. Meas.
Tech.*, 7, 647–687, doi:10.5194/amt-7-647-2014, 2014.

32



- 1 Belikov, D. A., Maksyutov, S., Sherlock, V., Aoki, S., Deutscher, N. M., Dohe, S., Griffith,
2 D., Kyro, E., Morino, I., Nakazawa, T., Notholt, J., Rettinger, M., Schneider, M., Sussmann,
3 R., Toon, G. C., Wennberg, P. O., and Wunch, D.: Simulations of column-averaged CO₂ and
4 CH₄ using the NIES TM with a hybrid sigma-isentropic (σ - θ) vertical coordinate, Atmos.
5 Chem. Phys., 13, 1713-1732, doi:10.5194/acp-13-1713-2013, 2013.
- 6
- 7 Biraud, S. C., Torn, M. S., Smith, J. R., Sweeney, C., Riley, W. J., and Tans, P. P.: A multi-
8 year record of airborne CO₂ observations in the US Southern Great Plains, Atmos. Meas.
9 Tech., 6, 751-763, doi:10.5194/amt-6-751-2013, 2013.
- 10
- 11 Crisp, D., Fisher, B. M., O'Dell, C., Frankenberg, C., Basilio, R., Bösch, H., Brown, L. R.,
12 Castano, R., Connor, B., Deutscher, N. M., Eldering, A., Griffith, D., Gunson, M., Kuze, A.,
13 Mandrake, L., McDuffie, J., Messerschmidt, J., Miller, C. E., Morino, I., Natraj, V., Notholt,
14 J., O'Brien, D. M., Oyafuso, F., Polonsky, I., Robinson, J., Salawitch, R., Sherlock, V., Smyth,
15 M., Suto, H., Taylor, T. E., Thompson, D. R., Wennberg, P. O., Wunch, D., and Yung, Y. L.:
16 The ACOS CO₂ retrieval algorithm – Part II: Global XCO₂ data characterization, Atmos.
17 Meas. Tech., 5, 687-707, doi:10.5194/amt-5-687-2012, 2012.
- 18
- 19 Deng, F., Jones, D. B. A., Henze, D. K., Bousserez, N., Bowman, K. W., Fisher, J. B., Nassar,
20 R., O'Dell, C., Wunch, D., Wennberg, P. O., Kort, E. A., Wofsy, S. C., Blumenstock, T.,
21 Deutscher, N. M., Griffith, D. W. T., Hase, F., Heikkinen, P., Sherlock, V., Strong, K.,
22 Sussmann, R., and Warneke, T.: Inferring regional sources and sinks of atmospheric CO₂
23 from GOSAT XCO₂ data, Atmos. Chem. Phys., 14, 3703-3727, doi:10.5194/acp-14-3703-
24 2014, 2014.
- 25
- 26 Deutscher, N. M., Griffith, D. W. T., Bryant, G. W., Wennberg, P. O., Toon, G. C.,
27 Washenfelder, R. A., Keppel-Aleks, G., Wunch, D., Yavin, Y., Allen, N. T., Blavier, J.-F.,
28 Jiménez, R., Daube, B. C., Bright, A. V., Matross, D. M., Wofsy, S. C., and Park, S.: Total
29 column CO₂ measurements at Darwin, Australia – site description and calibration against in
30 situ aircraft profiles, Atmos. Meas. Tech., 3, 947-958, doi:10.5194/amt-3-947-2010, 2010.



1

2 Deutscher, N. M., Sherlock, V., Mikaloff Fletcher, S. E., Griffith, D. W. T., Notholt, J.,
3 Macatangay, R., Connor, B. J., Robinson, J., Shiona, H., Velazco, V. A., Wang, Y.,
4 Wennberg, P. O., and Wunch, D.: Drivers of column-average CO₂ variability at Southern
5 Hemispheric Total Carbon Column Observing Network sites, *Atmos. Chem. Phys.*, 14, 9883-
6 9901, doi:10.5194/acp-14-9883-2014, 2014.

7

8 Dils, B., De Mazière, M., Müller, J. F., Blumenstock, T., Buchwitz, M., de Beek, R.,
9 Demoulin, P., Duchatelet, P., Fast, H., Frankenberg, C., Gloudemans, A., Griffith, D., Jones,
10 N., Kerzenmacher, T., Kramer, I., Mahieu, E., Mellqvist, J., Mittermeier, R. L., Notholt, J.,
11 Rinsland, C. P., Schrijver, H., Smale, D., Strandberg, A., Straume, A. G., Stremme, W.,
12 Strong, K., Sussmann, R., Taylor, J., van den Broek, M., Velazco, V., Wagner, T., Warneke,
13 T., Wiacek, A., and Wood, S.: Comparisons between SCIAMACHY and ground-based FTIR
14 data for total columns of CO, CH₄, CO₂ and N₂O, *Atmos. Chem. Phys.*, 6, 1953-1976,
15 doi:10.5194/acp-6-1953-2006, 2006.

16

17 Dils, B., Buchwitz, M., Reuter, M., Schneising, O., Boesch, H., Parker, R., Guerlet, S., Aben,
18 I., Blumenstock, T., Burrows, J. P., Butz, A., Deutscher, N. M., Frankenberg, C., Hase, F.,
19 Hasekamp, O. P., Heymann, J., De Mazière, M., Notholt, J., Sussmann, R., Warneke, T.,
20 Griffith, D., Sherlock, V., and Wunch, D.: The Greenhouse Gas Climate Change Initiative
21 (GHG-CCI): comparative validation of GHG-CCI SCIAMACHY/ENVISAT and TANSO-
22 FTS/GOSAT CO₂ and CH₄ retrieval algorithm products with measurements from the TCCON,
23 *Atmos. Meas. Tech.*, 7, 1723-1744, doi:10.5194/amt-7-1723-2014, 2014.

24

25 Gavrilov, N. M., Makarova, M. V., Poberovskii, A. V., and Timofeyev, Yu. M.: Comparisons
26 of CH₄ ground-based FTIR measurements near Saint Petersburg with GOSAT observations,
27 *Atmos. Meas. Tech.*, 7, 1003-1010, doi:10.5194/amt-7-1003-2014, 2014.

28



- 1 Guerlet, S., Basu, S., Butz, A., Krol, M., Hahne, P., Houweling, S., Hasekamp, O. P., and
2 Aben, I.: Reduced carbon uptake during the 2010 Northern Hemisphere summer from
3 GOSAT, Geophys. Res. Lett., 40, 2378-2383, doi:10.1002/grl.50402, 2013.
- 4
- 5 Heymann, J., Bovensmann, H., Buchwitz, M., Burrows, J. P., Deutscher, N. M., Notholt, J.,
6 Rettiger, M., Reuter, M., Schneising, O., Sussmann, R., and Warneke, T.: SCIAMACHY
7 WFM-DOAS XCO₂: reduction of scattering related errors, Atmos. Meas. Tech., 5, 2375-2390,
8 doi:10.5194/amt-5-2375-2012, 2012.
- 9
- 10 Inoue, H. Y. and Matsueda, H.: Variations in atmospheric CO₂ at the Meteorological
11 Research Institute, Tsukuba, Japan, J. Atmos. Chem., 23, 137-161, 1996.
- 12
- 13 Inoue, H. Y. and Matsueda, H.: Measurements of atmospheric CO₂ from a meteorological
14 tower in Tsukuba, Japan, Tellus B, 53, 205-219, doi:10.1034/j.1600-0889.2001.01163.x, 2001.
- 15
- 16 Inoue, M., Morino, I., Uchino, O., Miyamoto, Y., Yoshida, Y., Yokota, T., Machida, T., Sawa,
17 Y., Matsueda, H., Sweeney, C., Tans, P. P., Andrews, A. E., Biraud, S. C., Tanaka, T.,
18 Kawakami, S., and Patra, P. K.: Validation of XCO₂ derived from SWIR spectra of GOSAT
19 TANSO-FTS with aircraft measurement data, Atmos. Chem. Phys., 13, 9771-9788,
20 doi:10.5194/acp-13-9771-2013, 2013.
- 21
- 22 Inoue, M., Morino, I., Uchino, O., Miyamoto, Y., Saeki, T., Yoshida, Y., Yokota, T.,
23 Sweeney, C., Tans, P. P., Biraud, S. C., Machida, T., Pittman, J. V., Kort, E. A., Tanaka, T.,
24 Kawakami, S., Sawa, Y., Tsuboi, K., and Matsueda, H.: Validation of XCH₄ derived from
25 SWIR spectra of GOSAT TANSO-FTS with aircraft measurement data, Atmos. Meas. Tech.,
26 7, 2987-3005, doi:10.5194/amt-7-2987-2014, 2014.
- 27
- 28 Ishizawa, M., Shirai, T., Inoue, M., Morino, I., Yoshida, Y., Zhuravlev, R., Ganshin, A.,
29 Belikov, D., Saito, M., Oda, T., Valsala, V., Uchino, O., Yokota, T., and Maksyutov, S.:



- 1 Impact of retrieval biases of GOSAT XCO₂ on the surface CO₂ flux estimates, Soon to be
2 submitted to J. Geophys. Res.
- 3
- 4 Ishizawa, M., Uchino, O., Morino, I., Inoue, M., Yoshida, Y., Mabuchi, K., Shirai, T.,
5 Tohjima, Y., Maksyutov, S., Ohyama, H., Kawakami, S., and Takizawa, A.: Large XCH₄
6 anomaly in summer 2013 over Northeast Asia observed by GOSAT, Atmos. Chem. Phys.
7 Discuss., 15, 24995-25020, doi:10.5194/acpd-15-24995-2015, 2015.
- 8
- 9 Kort, E. A., Wofsy, S. C., Daube, B. C., Diao, M., Elkins, J. W., Gao, R. S., Hintsa, E. J.,
10 Hurst, D. F., Jimenez, R., Moore, F. L., Spackman, J. R., and Zondlo, M. A.: Atmospheric
11 observations of Arctic Ocean methane emissions up to 82° north, Nature Geoscience, 5, 318-
12 321, doi:10.1038/ngeo1452, 2012.
- 13
- 14 Kuze, A., Suto, H., Nakajima, M., and Hamazaki, T.: Thermal and near infrared sensor for
15 carbon observation Fourier-transform spectrometer on the Greenhouse Gases Observing
16 Satellite for greenhouse gases monitoring, Applied Optics, 48, 6716-6733
17 doi:10.1364/AO.48.006716, 2009.
- 18
- 19 Machida, T., Nakazawa, T., Ishidoya, S., Maksyutov, S., Tohjima, Y., Takahashi, Y., Watai,
20 T., Vinnichenko, N., Panchenko, M., Arshinov, M., Fedoseev, N., and Inoue, G: Temporal
21 and spatial variations of atmospheric CO₂ mixing ratio over Siberia, Ext. Abstr. 6th
22 International CO₂ Conf., 1-5 October, Sendai, Japan, 2001.
- 23
- 24 Machida, T., Matsueda, H., Sawa, Y., Nakagawa, Y., Hirotani, K., Kondo, N., Goto, K.,
25 Nakazawa, T., Ishikawa, K., and Ogawa, T.: Worldwide measurements of atmospheric CO₂
26 and other trace gas species using commercial airlines, J. Atmos. Oceanic. Technol., 25, 1744-
27 1754, doi:10.1175/2008JTECHA1082.1, 2008.
- 28



- 1 Maksyutov, S., Takagi, H., Valsala, V. K., Saito, M., Oda, T., Saeki, T., Belikov, D. A., Saito,
2 R., Ito, A., Yoshida, Y., Morino, I., Uchino, O., Andres, R. J., and Yokota, T.: Regional CO₂
3 flux estimates for 2009–2010 based on GOSAT and ground-based CO₂ observations, *Atmos.*
4 *Chem. Phys.*, 13, 9351-9373, doi:10.5194/acp-13-9351-2013, 2013.
- 5
- 6 Messerschmidt, J., Macatangay, R., Notholt, J., Petri, C., Warneke, T., and Weinzierl, C.:
7 Side by side measurements of CO₂ by ground-based Fourier transform spectrometry (FTS),
8 *Tellus B*, 62, 749-758, doi:10.1111/j.1600-0889.2010.00491.x, 2010.
- 9
- 10 Miyamoto, Y., Inoue, M., Morino, I., Uchino, O., Yokota, T., Machida, T., Sawa, Y.,
11 Matsueda, H., Sweeney, C., Tans, P. P., Andrews, A. E., Biraud, S. C., and Patra, P. K.:
12 Atmospheric column-averaged mole fractions of carbon dioxide at 53 aircraft measurement
13 sites, *Atmos. Chem. Phys.*, 13, 5265-5275, doi:10.5194/acp-13-5265-2013, 2013.
- 14
- 15 Morino, I., Uchino, O., Inoue, M., Yoshida, Y., Yokota, T., Wennberg, P. O., Toon, G. C.,
16 Wunch, D., Roehl, C. M., Notholt, J., Warneke, T., Messerschmidt, J., Griffith D. W. T.,
17 Deutscher, N. M., Sherlock, V., Connor, B., Robinson, J., Sussmann, R., and Rettinger, M.:
18 Preliminary validation of column-averaged volume mixing ratios of carbon dioxide and
19 methane retrieved from GOSAT short-wavelength infrared spectra, *Atmos. Meas. Tech.*, 4,
20 1061-1076, doi:10.5194/amt-4-1061-2011, 2011.
- 21
- 22 Nakazawa, T., Sugawara, S., Inoue, G., Machida, T., Maksyutov, S., and Mukai, H.: Aircraft
23 measurements of the concentrations of CO₂, CH₄, N₂O, and CO and the carbon and oxygen
24 isotopic ratios of CO₂ in the troposphere over Russia, *J. Geophys. Res.*, 102, 3843-3859, 1997.
- 25
- 26 Nguyen, H., Osterman, G., Wunch, D., O'Dell, C., Mandrake, L., Wennberg, P., Fisher, B.,
27 and Castano, R.: A method for colocating satellite XCO₂ data to ground-based data and its
28 application to ACOS-GOSAT and TCCON, *Atmos. Meas. Tech.*, 7, 2631-2644,
29 doi:10.5194/amt-7-2631-2014, 2014.
- 30



- 1 O'Dell, C. W., Connor, B., Bösch, H., O'Brien, D., Frankenberg, C., Castano, R., Christi, M.,
2 Eldering, D., Fisher, B., Gunson, M., McDuffie, J., Miller, C. E., Natraj, V., Oyafuso, F.,
3 Polonsky, I., Smyth, M., Taylor, T., Toon, G. C., Wennberg, P. O., and Wunch, D.: The
4 ACOS CO₂ retrieval algorithm – Part 1: Description and validation against synthetic
5 observations, *Atmos. Meas. Tech.*, 5, 99-121, doi:10.5194/amt-5-99-2012, 2012.
- 6
- 7 Oshchepkov, S., Bril, A., Yokota, T., Wennberg, P. O., Deutscher, N. M., Wunch, D., Toon,
8 G. C., Yoshida, Y., O'Dell, C. W., Crisp, D., Miller, C. E., Frankenberg, C., Butz, A., Aben, I.,
9 Guerlet, S., Hasekamp, O., Boesch, H., Cogan, A., Parker, R., Griffith, D., Macatangay, R.,
10 Notholt, J., Sussmann, R., Rettinger, M., Sherlock, V., Robinson, J., Kyrö, E., Heikkinen, P.,
11 Feist, D. G., Morino, I., Kadygrov, N., Belikov, D., Maksyutov, S., Matsunaga, T., Uchino,
12 O., and Watanabe, H.: Effects of atmospheric light scattering on spectroscopic observations of
13 greenhouse gases from space. Part 2: Algorithm intercomparison in the GOSAT data
14 processing for CO₂ retrievals over TCCON sites, *J. Geophys. Res.*, 118, 1493-1512,
15 doi:10.1002/jgrd.50146, 2013.
- 16
- 17 Saito, R., Patra, P. K., Deutscher, N., Wunch, D., Ishijima, K., Sherlock, V., Blumenstock, T.,
18 Dohe, S., Griffith, D., Hase, F., Heikkinen, P., Kyrö, E., Macatangay, R., Mendonca, J.,
19 Messerschmidt, J., Morino, I., Notholt, J., Rettinger, M., Strong, K., Sussmann, R., and
20 Warneke, T.: Technical Note: Latitude-time variations of atmospheric column-average dry air
21 mole fractions of CO₂, CH₄ and N₂O, *Atmos. Chem. Phys.*, 12, 7767-7777, doi:10.5194/acp-
22 12-7767-2012, 2012.
- 23
- 24 Saitoh, N., Touno, M., Hayashida, S., Imasu, R., Shiomi, K., Yokota, T., Yoshida, Y.,
25 Machida, T., Matsueda, H., and Sawa, Y.: Comparisons between XCH₄ from GOSAT
26 Shortwave and Thermal Infrared Spectra and Aircraft CH₄ Measurement over Guam, *Sci.*
27 *Online Lett. Atmos. (SOLA)*, 8, 145-149, doi:10.2151/sola.2012-036, 2012.
- 28
- 29 Santoni, G. W., Daube, B. C., Kort, E. A., Jiménez, R., Park, S., Pittman, J. V., Gottlieb, E.,
30 Xiang, B., Zahniser, M. S., Nelson, D. D., McManus, J. B., Peischl, J., Ryerson, T. B.,
31 Holloway, J. S., Andrews, A. E., Sweeney, C., Hall, B., Hintsa, E. J., Moore, F. L., Elkins, J.



- 1 W., Hurst, D. F., Stephens, B. B., Bent, J., and Wofsy, S. C.: Evaluation of the airborne
2 quantum cascade laser spectrometer (QCLS) measurements of the carbon and greenhouse gas
3 suite – CO₂, CH₄, N₂O, and CO – during the CalNex and HIPPO campaigns, *Atmos. Meas.*
4 *Tech.*, 7, 1509-1526, doi:10.5194/amt-7-1509-2014, 2014.
- 5
- 6 Scheepmaker, R. A., Frankenberg, C., Deutscher, N. M., Schneider, M., Barthlott, S.,
7 Blumenstock, T., Garcia, O. E., Hase, F., Jones, N., Mahieu, E., Notholt, J., Velazco, V.,
8 Landgraf, J., and Aben, I.: Validation of SCIAMACHY HDO/H₂O measurements using the
9 TCCON and NDACC-MUSICA networks, *Atmos. Meas. Tech.*, 8, 1799-1818,
10 doi:10.5194/amt-8-1799-2015, 2015.
- 11
- 12 Schmid, B., Tomlinson, J. M., Hubbe, J. M., Comstock, J. M., Mei, F., Chand, D., Pekour, M.
13 S., Kluzek, C. D., Andrews, E., Biraud, S. C., and McFarquhar, G. M.: The DOE ARM Aerial
14 Facility. *Bull. Amer. Meteor. Soc.*, 95, 723-742, doi:10.1175/BAMS-D-13-00040.1, 2014.
- 15
- 16 Schneising, O., Bergamaschi, P., Bovensmann, H., Buchwitz, M., Burrows, J. P., Deutscher,
17 N. M., Griffith, D. W. T., Heymann, J., Macatangay, R., Messerschmidt, J., Notholt, J.,
18 Rettinger, M., Reuter, M., Sussmann, R., Velazco, V. A., Warneke, T., Wennberg, P. O., and
19 Wunch, D.: Atmospheric greenhouse gases retrieved from SCIAMACHY: comparison to
20 ground-based FTS measurements and model results, *Atmos. Chem. Phys.*, 12, 1527-1540,
21 doi:10.5194/acp-12-1527-2012, 2012.
- 22
- 23 Schneising, O., Heymann, J., Buchwitz, M., Reuter, M., Bovensmann, H., and Burrows, J. P.:
24 Anthropogenic carbon dioxide source areas observed from space: assessment of regional
25 enhancements and trends, *Atmos. Chem. Phys.*, 13, 2445-2454, doi:10.5194/acp-13-2445-
26 2013, 2013.
- 27
- 28 Sweeney, C., Karion, A., Wolter, S., Newberger, T., Guenther, D., Higgs, J. A., Andrews, A.
29 E., Lang, P. M., Neff, D., Dlugokencky, E., Miller, J. B., Montzka, S. A., Miller, B. R.,
30 Masarie, K. A., Biraud, S. C., Novelli, P. C., Crotwell, M., Crotwell, A. M., Thoning, K., and



- 1 Tans, P. P.: Seasonal climatology of CO₂ across North America from aircraft measurements
2 in the NOAA/ESRL Global Greenhouse Gas Reference Network, J. Geophys. Res., 120,
3 5155-5190, doi:10.1002/2014JD022591, 2015.
- 4
- 5 Takagi, H., Saeki, T., Oda, T., Saito, M., Valsala, V., Belikov, D., Saito, R., Yoshida, Y.,
6 Morino, I., Uchino, O., Andres, R. J., Yokota T., and Maksyutov, S.: On the Benefit of
7 GOSAT Observations to the Estimation of Regional CO₂ Fluxes, Sci. Online Lett. Atmos.
8 (SOLA), 7, 161-164, doi:10.2151/sola.2011-041, 2011.
- 9
- 10 Tanaka, T., Miyamoto, Y., Morino, I., Machida, T., Nagahama, T., Sawa, Y., Matsueda, H.,
11 Wunch, D., Kawakami, S., and Uchino, O.: Aircraft measurements of carbon dioxide and
12 methane for the calibration of ground-based high-resolution Fourier Transform Spectrometers
13 and a comparison to GOSAT data measured over Tsukuba and Moshiri, Atmos. Meas. Tech.,
14 5, 2003-2012, doi:10.5194/amt-5-2003-2012, 2012.
- 15
- 16 Tsuboi, K., Matsueda, H., Sawa, Y., Niwa, Y., Nakamura, M., Kuboike, D., Saito, K., Ohmori,
17 H., Iwatsubo, S., Nishi, H., Hanamiya, Y., Tsuji, K., and Baba, Y.: Evaluation of a new JMA
18 aircraft flask sampling system and laboratory trace gas analysis system, Atmos. Meas. Tech.,
19 6, 1257-1270, doi:10.5194/amt-6-1257-2013, 2013.
- 20
- 21 Uchino, O., Kikuchi, N., Sakai, T., Morino, I., Yoshida, Y., Nagai, T., Shimizu, A., Shibata,
22 T., Yamazaki, A., Uchiyama, A., Kikuchi, N., Oshchepkov, S., Bril, A., and Yokota, T.:
23 Influence of aerosols and thin cirrus clouds on the GOSAT-observed CO₂: a case study over
24 Tsukuba, Atmos. Chem. Phys., 12, 3393-3404, doi:10.5194/acp-12-3393-2012, 2012.
- 25
- 26 WMO: WMO Greenhouse Gas Bulletin, The State of Greenhouse Gases in the Atmosphere
27 Using Global Observations through 2007, No. 4, World Meteorological Organization, 2008,
28 available at: <http://www.wmo.int/pages/prog/arep/gaw/ghg/GHGbulletin.html> (last access:
29 January 2015).
- 30



- 1 WMO: WMO Greenhouse Gas Bulletin, The State of Greenhouse Gases in the Atmosphere
2 Based on Global Observations through 2013, No. 10, World Meteorological Organization,
3 2014, available at: <http://www.wmo.int/pages/prog/arep/gaw/ghg/GHGbulletin.html> (last
4 access: January 2015).
- 5
- 6 Wofsy, S. C. and the HIPPO Science Team and Cooperating Modellers and Satellite Teams:
7 HIAPER Pole-to-Pole Observations (HIPPO): fine-grained, global-scale measurements of
8 climatically important atmospheric gases and aerosols, Philos. T. Roy. Soc. A, 369, 2073-
9 2086, doi:10.1098/rsta.2010.0313, 2011.
- 10
- 11 Wofsy, S. C., Daube, B. C., Jimenez, R., Kort, E., Pittman, J. V., Park, S., Commane, R.,
12 Xiang, B., Santoni, G., Jacob, D., Fisher, J., Pickett-Heaps, C., Wang, H., Wecht, K., Wang,
13 Q.-Q., Stephens, B. B., Shertz, S., Watt, A. S., Romashkin, P., Campos, T., Haggerty, J.,
14 Cooper, W. A., Rogers, D., Beaton, S., Hendershot, R., Elkins, J. W., Fahey, D. W., Gao, R.
15 S., Moore, F., Montzka, S. A., Schwarz, J. P., Perring, A. E., Hurst, D., Miller, B. R.,
16 Sweeney, C., Oltmans, S., Nance, D., Hints, E., Dutton, G., Watts, L. A., Spackman, J. R.,
17 Rosenlof, K. H., Ray, E. A., Hall, B., Zondlo, M. A., Diao, M., Keeling, R., Bent, J., Atlas, E.
18 L., Lueb, R., and Mahoney, M. J.: HIPPO merged 10-second Meteorology, Atmospheric
19 Chemistry, Aerosol Data (R_20121129), used data file
20 "HIPPO_all_missions_merged_10s_20121129.tbl", Carbon Dioxide Information Analysis
21 Center, Oak Ridge National Laboratory, Oak Ridge, Tennessee, U.S.A.
22 http://dx.doi.org/10.3334/CDIAC/hippo_010, (last access: July 2013), 2012.
- 23
- 24 Wunch, D., Wennberg, P. O., Toon, G. C., Keppel-Aleks, G., and Yavin, Y. G.: Emissions of
25 greenhouse gases from a North American megacity, Geophys. Res. Lett., 36, L15810,
26 doi:10.1029/2009GL039825, 2009.
- 27
- 28 Wunch, D., Toon, G. C., Wennberg, P. O., Wofsy, S. C., Stephens, B. B., Fischer, M. L.,
29 Uchino, O., Abshire, J. B., Bernath, P., Biraud, S. C., Blavier, J.-F. L., Boone, C., Bowman, K.
30 P., Browell, E. V., Campos, T., Connor, B. J., Daube, B. C., Deutscher, N. M., Diao, M.,
31 Elkins, J. W., Gerbig, C., Gottlieb, E., Griffith, D. W. T., Hurst, D. F., Jiménez, R., Keppel-



- 1 Aleks, G., Kort, E. A., Macatangay, R., Machida, T., Matsueda, H., Moore, F., Morino, I.,
2 Park, S., Robinson, J., Roehl, C. M., Sawa, Y., Sherlock, V., Sweeney, C., Tanaka, T., and
3 Zondlo, M. A.: Calibration of the Total Carbon Column Observing Network using aircraft
4 profile data, *Atmos. Meas. Tech.*, 3, 1351-1362, doi:10.5194/amt-3-1351-2010, 2010.
- 5
- 6 Wunch, D., Toon, G. C., Blavier, J.-F. L., Washenfelder, R. A., Notholt, J., Connor, B. J.,
7 Griffith, D. W. T., Sherlock, V., and Wennberg, P. O.: The Total Carbon Column Observing
8 Network, *Phil. Trans. R. Soc. A*, 369, 2087-2112, doi:10.1098/rsta.2010.0240, 2011a.
- 9
- 10 Wunch, D., Wennberg, P. O., Toon, G. C., Connor, B. J., Fisher, B., Osterman, G. B.,
11 Frankenberg, C., Mandrake, L., O'Dell, C., Ahonen, P., Biraud, S. C., Castano, R., Cressie,
12 N., Crisp, D., Deutscher, N. M., Eldering, A., Fisher, M. L., Griffith, D. W. T., Gunson, M.,
13 Heikkinen, P., Keppel-Aleks, G., Kyrö, E., Lindenmaier, R., Macatangay, R., Mendonca, J.,
14 Messerschmidt, J., Miller, C. E., Morino, I., Notholt, J., Oyafuso, F. A., Rettinger, M.,
15 Robinson, J., Roehl, C. M., Salawitch, R. J., Sherlock, V., Strong, K., Sussmann, R., Tanaka,
16 T., Thompson, D. R., Uchino, O., Warneke, T., and Wofsy, S. C.: A method for evaluating
17 bias in global measurements of CO₂ total columns from space, *Atmos. Chem. Phys.*, 11,
18 12317-12337, doi:10.5194/acp-11-12317-2011, 2011b.
- 19
- 20 Wunch, D., Toon, G. C., Sherlock, V., Deutscher, N. M., Liu, X., Feist, D. G., and Wennberg,
21 P. O.: The Total Carbon Column Observing Network's GGG2014 Data Version. Carbon
22 Dioxide Information Analysis Center, Oak Ridge National Laboratory, Oak Ridge, Tennessee,
23 U.S.A. doi: 10.14291/tcco.2014.documentation.R0/1221662, 2015.
- 24
- 25 Xiong, X., Barnet, C., Maddy, E., Sweeney, C., Liu, X., Zhou, L., and Goldberg, M.:
26 Characterization and validation of methane products from the Atmospheric Infrared Sounder
27 (AIRS), *J. Geophys. Res.*, 113, G00A01, doi:10.1029/2007JG000500, 2008.
- 28



- 1 Yokota, T., Yoshida, Y., Eguchi, N., Ota, Y., Tanaka, T., Watanabe, H., and Maksyutov, S.:
2 Global Concentrations of CO₂ and CH₄ Retrieved from GOSAT: First Preliminary Results,
3 Sci. Online Lett. Atmos. (SOLA), 5, 160-163, doi:10.2151/sola.2009-041, 2009.
- 4
- 5 Yoshida, Y., Ota, Y., Eguchi, N., Kikuchi, N., Nobuta, K., Tran, H., Morino, I., and Yokota,
6 T.: Retrieval algorithm for CO₂ and CH₄ column abundances from short-wavelength infrared
7 spectral observations by the Greenhouse gases observing satellite, Atmos. Meas. Tech., 4,
8 717-734, doi:10.5194/amt-4-717-2011, 2011.
- 9
- 10 Yoshida, Y., Kikuchi, N., Morino, I., Uchino, O., Oshchepkov, S., Bril, A., Saeki, T.,
11 Schutgens, N., Toon, G. C., Wunch, D., Roehl, C. M., Wennberg, P. O., Griffith, D. W. T.,
12 Deutscher, N. M., Warneke, T., Notholt, J., Robinson, J., Sherlock, V., Connor, B., Rettinger,
13 M., Sussmann, R., Ahonen, P., Heikkinen, P., Kyrö, E., Mendonca, J., Strong, K., Hase, F.,
14 Dohe, S., and Yokota, T.: Improvement of the retrieval algorithm for GOSAT SWIR XCO₂
15 and XCH₄ and their validation using TCCON data, Atmos. Meas. Tech., 6, 1533-1547,
16 doi:10.5194/amt-6-1533-2013, 2013.
- 17



1 Table 1. Basic information on the TCCON sites used for correction and validation of the
 2 GOSAT data.

3

site	latitude [deg. N]	longitude [deg. E]	elevation [m]	region	data reference (DOI number)
Ny Ålesund	78.90	11.90	20	Spitzbergen, Norway	10.14291/tccon.ggg2014. nyalesund01.R0/1149278
Sodankylä	67.37	26.63	188	Finland	10.14291/tccon.ggg2014. sodankyla01.R0/1149280
Białystok	53.23	23.03	180	Poland	10.14291/tccon.ggg2014. bialystok01.R1/1183984
Bremen	53.10	8.85	27	Germany	10.14291/tccon.ggg2014. bremen01.R0/1149275
Karlsruhe	49.10	8.44	120	Germany	10.14291/tccon.ggg2014. karlsruhe01.R1/1182416
Orléans	47.97	2.11	130	France	10.14291/tccon.ggg2014. orleans01.R0/1149276
Garmisch	47.48	11.06	740	Germany	10.14291/tccon.ggg2014. garmisch01.R0/1149299
Park Falls	45.95	-90.27	472	United States	10.14291/tccon.ggg2014. parkfalls01.R0/1149161
Rikubetsu	43.46	143.77	361	Japan	10.14291/tccon.ggg2014. rikubetsu01.R0/1149282
Indianapolis	39.86	-86.00	270	United States	10.14291/tccon.ggg2014. indianapolis01.R0/1149164
Four Corners	36.80	-108.48	1643	United States	10.14291/tccon.ggg2014. fourcorners01.R0/1149272
Lamont	36.60	-97.49	320	United States	10.14291/tccon.ggg2014. lamont01.R0/1149159
(120HR)					
Tsukuba	36.05	140.12	30	Japan	10.14291/tccon.ggg2014. tsukuba01.R0/1149281
(125HR)					
Edwards	34.96	-117.88	700	United States	10.14291/tccon.ggg2014. edwards01.R0/1149289
JPL	34.20	-118.18	390	United States	10.14291/tccon.ggg2014. jpl02.R0/1149297
Pasadena	34.14	-118.13	237	United States	10.14291/tccon.ggg2014. pasadena01.R1/1182415
Saga	33.24	130.29	7	Japan	10.14291/tccon.ggg2014. saga01.R0/1149283
Izaña	28.30	-16.50	2370	Tenerife, Canary Islands	10.14291/tccon.ggg2014. izana01.R0/1149295
Ascension Island	-7.92	-14.33	31	South Atlantic Ocean	10.14291/tccon.ggg2014. ascension01.R0/1149285
Darwin	-12.42	130.89	30	Australia	10.14291/tccon.ggg2014. darwin01.R0/1149290



Reunion Island	-20.90	55.49	87	Indian Ocean	10.14291/tccon.ggg2014. reunion01.R0/1149288
Wollongong	-34.41	150.88	30	Australia	10.14291/tccon.ggg2014. wollongong01.R0/1149291 (120HR)
Lauder	-45.04	169.68	370	New Zealand	10.14291/tccon.ggg2014. lauder01.R0/1149293 (125HR) 10.14291/tccon.ggg2014. lauder02.R0/1149298

1
2
3
4
5
6
7
8
9
10
11
12
13
14
15
16
17
18
19



1 Table 2. Basic information on the aircraft observation sites used for validation of the GOSAT
 2 data.

(a) CONTRAIL

site code	latitude [deg. N]	longitude [deg. E]	elevation [m]	region	site name
LHR	51.5	-0.5	24	London	Heathrow Airport
YVR	49.2	-123.2	4	Vancouver	Vancouver International Airport
MXP	45.6	8.7	24	Milan	Milan Malpensa International Airport
FCO	41.8	12.3	5	Rome	Fiumicino Airport
ICN	37.5	126.5	7	Incheon	Incheon International Airport
NRT	35.8	140.4	43	Narita	Narita International Airport
HND	35.6	139.8	6	Haneda	Tokyo International Airport
NGO	34.9	136.8	5	Nagoya	Chubu Centrair International Airport
KIX	34.4	135.2	0	Kansai	Kansai International Airport
HNL	21.3	-157.9	4	Honolulu	Honolulu International Airport
BKK	13.7	100.7	2	Bangkok	Suvarnabhumi International Airport
SIN	1.4	104.0	7	Singapore	Singapore Changi International Airport
CGK	-6.1	106.7	10	Jakarta	Jakarta International Soekarno-Hatta Airport
SYD	-33.9	151.2	6	Sydney	Kingsford Smith Airport

(b) NOAA

site code	latitude [deg. N]	longitude [deg. E]	elevation [m]	region	site name
DND	48.4	-97.8	464	United States	Dahlen, North Dakota
LEF	45.9	-90.3	472	United States	Park Falls, Wisconsin
NHA	43.0	-70.6	0	United States	Worcester, Massachusetts
WBI	41.7	-91.4	242	United States	West Branch, Iowa
THD	41.1	-124.2	107	United States	Trinidad Head, California
BNE	40.8	-97.2	466	United States	Beaver Crossing, Nebraska
CAR	40.4	-104.3	1740	United States	Briggsdale, Colorado
HIL	40.1	-87.9	202	United States	Homer, Illinois
AAO	40.1	-88.6	213	United States	Airborne Aerosol Observing, Illinois
SCA	32.8	-79.6	0	United States	Charleston, South Carolina
TGC	27.7	-96.9	0	United States	Sinton, Texas



RTA	-21.3	-159.8	3	Cook Islands	Rarotonga
-----	-------	--------	---	--------------	-----------

(c) DOE

site code	latitude [deg. N]	longitude [deg. E]	elevation [m]	region	site name
SGP	36.8	-97.5	314	United States	Southern Great Plains, Oklahoma

(d) NIES

site code	latitude [deg. N]	longitude [deg. E]	elevation [m]	region	site name
YAK	62	130	136	Russia	Yakutsk
SGM	35.1	139.3	0	Japan	Sagami-bay

(e) JMA

site code	latitude [deg. N]	longitude [deg. E]	elevation [m]	region	site name
MNM	24.3	154.0	8	Japan	Minamitorishima

1

(f) HIPPO

site code	latitude [deg. N]	longitude [deg. E]	elevation [m]	region	site name
HPA	49	-110	1040	United States	northeastern part of Great Falls, Montana
HPB	-28	-166	0	South Pacific Ocean	southwestern part of Rarotonga
HPC	-23	-161	0	South Pacific Ocean	southwestern part of Rarotonga
HPD	-33	158	0	Australia	eastern part of Lord Howe
HPE	-33	152	0	Australia	east coast of Newcastle
HPF	-20	156	0	Coral Sea	western part of Chesterfield Islands
HPG	-5	-167	0	Kiribati	western part of Enderbury
HPH	-37	179	0	New Zealand	northeastern part of Bay of Plenty
HPI	-36	179	0	New Zealand	northeastern part of Bay of Plenty

2

(g)
NIES-JAXA

site code	latitude [deg. N]	longitude [deg. E]	elevation [m]	region	site name
TKB	36.1	140.1	31	Japan	Tsukuba



1 Table 3. Values and errors of the regression coefficients for (a) XCO₂ and (b) XCH₄ retrievals
2 calculated by multiple linear regression. The units of C₀, C₁, C₂, C₃, and C₄ for XCO₂ are
3 [ppm], [ppm/units of AOD], [ppm/hPa], [ppm/airmass], and [ppm/units of albedo],
4 respectively. The units of C₀ and C₁ for XCH₄ are [ppb] and [ppb/units of AOD], respectively.

5 (a)
6

coefficients	Land		Ocean	
	Values	Errors	Values	Errors
C ₀	0.865	0.021	1.903	0.055
C ₁	-7.793	1.357	15.493	2.725
C ₂	-0.282	0.006	-0.237	0.013
C ₃	0.023	0.064	8.602	1.060
C ₄	-2.036	0.433	—	—

7
8 (b)
9

	Land		Ocean	
	Values	Errors	Values	Errors
C ₀	6.0	0.2	0.2	0.6
C ₁	45.8	10.0	103.0	26.4

10
11
12



1 Table 4. The average and standard deviation of the differences between uncorrected/corrected
 2 GOSAT XCO₂ and TCCON XCO₂ at each TCCON site. The GOSAT data were retrieved
 3 over (a) land and (b) ocean regions within ±5° latitude/longitude boxes centered at each site.
 4 The averages and standard deviations of the differences of the matched data at all TCCON
 5 sites (single scan) and those of the station biases are also shown in the second row from the
 6 bottom and the bottom row of the table, respectively.

7 (a)
 8

Land	Differences between uncorrected XCO ₂ and TCCON XCO ₂		Differences between corrected GOSAT XCO ₂ and TCCON XCO ₂	
	site	number	average [ppm]	SD [ppm]
Sodankylä	152	-0.03	1.93	0.48
Białystok	305	-0.18	2.22	0.79
Bremen	62	-0.10	1.98	0.46
Karlsruhe	229	0.35	2.27	0.85
Orléans	402	-0.26	2.00	0.24
Garmisch	326	0.23	2.42	0.70
Park Falls	482	-0.50	2.15	0.37
Rikubetsu	7	-0.92	1.32	-0.46
Indianapolis	158	-0.03	1.69	0.37
Four Corners	142	-1.17	1.95	0.07
Lamont	2767	-1.72	1.79	-0.49
Tsukuba	419	1.55	2.37	1.67
Edwards	38	-1.35	1.46	-0.49
JPL	264	-2.32	2.32	-1.01
Pasadena	109	-0.41	2.12	0.22
Saga	128	0.37	2.37	0.66
Izaña	56	0.47	1.34	0.92
Darwin	926	-1.16	1.51	-0.25
Wollongong	1071	-0.68	2.25	-0.05
Lauder	202	-0.77	1.79	-0.23
Total (single scan)	8245	-0.86	2.18	0.00
Total (station bias)	20	-0.43	0.87	0.24
				0.62



1

2

(b)

3

4

Ocean	Differences between uncorrected GOSAT XCO ₂ and TCCON XCO ₂			Differences between corrected GOSAT XCO ₂ and TCCON XCO ₂		
	site	number	average [ppm]	SD [ppm]	average [ppm]	SD [ppm]
Garmisch	5	-0.55	0.49	-0.67	0.83	
Tsukuba	2	-2.87	2.35	-4.01	0.65	
JPL	8	-4.71	3.64	-1.36	2.47	
Saga	14	-1.15	2.56	-0.34	1.56	
Izana	50	-1.50	1.36	0.23	1.17	
Ascension Island	234	-1.93	1.62	-0.17	1.18	
Darwin	85	-1.64	1.86	0.54	1.56	
Reunion Island	43	-2.19	1.43	-0.08	0.95	
Wollongong	97	-2.04	1.49	0.05	1.04	
Lauder	6	-2.54	2.32	0.53	0.87	
Total (single scan)	544	-1.90	1.72	-0.01	1.29	
Total (station bias)	10	-2.11	1.13	-0.53	1.35	

5

6

7

8

9

10

11

12

13

14



1 Table 5. The average and standard deviation of the differences between uncorrected/corrected
 2 GOSAT XCH₄ and TCCON XCH₄ at each TCCON site. The GOSAT data were retrieved
 3 over (a) land and (b) ocean regions within ±5° latitude/longitude boxes centered at each site.
 4 The averages and standard deviations of the differences of the matched data at all TCCON
 5 sites (single scan) and those of the station biases are also shown in the second row from the
 6 bottom and the bottom row of the table, respectively.

7

8 (a)

Land	Differences between uncorrected GOSAT XCH ₄ and TCCON XCH ₄			Differences between corrected GOSAT XCH ₄ and TCCON XCH ₄		
	site	number	average [ppb]	SD [ppb]	average [ppb]	SD [ppb]
Sodankylä	152	-2.3	11.4	3.8	11.4	
Białystok	305	0.5	12.9	6.2	12.9	
Bremen	62	-1.6	12.7	4.2	12.7	
Karlsruhe	229	-0.9	15.3	5.0	15.3	
Orléans	402	-3.9	12.7	2.0	12.7	
Garmisch	326	6.2	16.3	11.9	16.3	
Park Falls	482	3.3	13.9	9.2	13.9	
Rikubetsu	7	4.1	8.6	9.7	8.8	
Indianapolis	158	-1.4	10.9	5.0	10.9	
Four Corners	142	-8.9	14.2	-3.0	14.3	
Lamont	2767	-9.0	15.1	-2.9	15.2	
Tsukuba	419	1.9	13.2	7.5	13.1	
Edwards	38	-19.5	16.8	-13.2	16.7	
JPL	264	-21.1	19.4	-15.1	19.4	
Pasadena	109	-8.1	15.3	-1.8	15.3	
Saga	128	-5.3	14.4	0.0	14.4	
Izana	56	15.4	12.7	20.1	13.1	
Darwin	926	-8.6	8.9	-2.4	9.1	
Wollongong	1076	-9.1	14.5	-2.8	14.7	
Lauder	208	-3.9	11.3	2.4	11.2	
Total (single scan)	8256	-6.0	15.2	0.0	15.2	
Total (station bias)	20	-3.6	8.4	2.3	8.1	

9



1

2 (b)

3

Ocean	Differences between uncorrected GOSAT XCH ₄ and TCCON XCH ₄			Differences between corrected GOSAT XCH ₄ and TCCON XCH ₄		
	site	number	average [ppb]	SD [ppb]	average [ppb]	SD [ppb]
Garmisch	5	18.7	11.0	20.4	11.0	
Tsukuba	2	21.9	16.0	21.2	17.2	
JPL	8	-17.1	13.1	-17.4	12.9	
Saga	14	0.7	17.0	-0.3	17.0	
Izana	50	14.8	7.7	14.1	8.4	
Ascension Island	234	-1.0	11.5	-0.6	11.2	
Darwin	85	4.1	13.2	3.0	13.3	
Reunion Island	43	-0.4	8.3	0.1	8.9	
Wollongong	97	-9.7	11.1	-8.6	11.7	
Lauder	6	-5.9	11.9	-4.3	12.3	
Total (single scan)	544	-0.2	13.4	-0.1	13.2	
Total (station bias)	10	2.6	12.6	2.8	12.5	

4

5

6

7

8

9

10

11

12

13



1 Table 6. The average and standard deviation of the differences between uncorrected/corrected
 2 GOSAT XCO₂ and aircraft-based XCO₂ at each aircraft observation site. The GOSAT data
 3 were retrieved over (a) land and (b) ocean regions within $\pm 5^\circ$ latitude/longitude boxes
 4 centered at each site. The averages and standard deviations of the differences of the matched
 5 data at all aircraft observation sites (single scan) and those of the station biases are also shown
 6 in the second row from the bottom and the bottom row of the table, respectively.

7

8

(a)

9

10

Land		Differences between uncorrected GOSAT XCO ₂ and aircraft-based XCO ₂		Differences between corrected GOSAT XCO ₂ and aircraft-based XCO ₂	
Site	number	average [ppm]	SD [ppm]	average [ppm]	SD [ppm]
LHR	3	-3.24	1.25	-2.09	0.66
YVR	7	-0.64	2.07	0.21	1.95
MXP	2	0.06	1.88	1.09	1.54
ICN	1	0.64	—	3.37	—
NRT	69	0.17	2.52	0.54	2.34
HND	2	-0.38	2.56	0.09	3.83
NGO	15	0.27	2.47	0.73	2.39
KIX	5	-1.01	3.25	-0.19	2.73
BKK	5	-2.90	3.86	-1.78	3.43
SYD	22	-1.19	2.48	-0.62	2.19
DND	11	-1.37	1.74	-0.47	1.48
LEF	34	0.02	2.77	0.66	2.79
NHA	25	0.27	1.64	0.44	1.69
WBI	23	-0.95	2.92	0.17	2.43
THD	4	-1.99	1.64	-0.06	1.13
BNE	6	-1.15	2.48	0.15	2.02
CAR	51	-2.17	2.20	-0.73	1.93
HIL	37	-2.16	1.96	-1.25	2.33
AAO	20	-0.18	2.32	0.64	2.28



SCA	22	-0.31	1.56	-0.01	1.60
TGC	15	-0.51	2.53	0.45	3.02
SGP	68	-1.61	2.20	-0.43	2.03
YAK	3	1.70	2.89	1.79	2.59
SGM	6	1.02	3.11	1.63	2.71
HPA	1	-2.84	—	-0.76	—
HPH	1	-1.91	—	-0.71	—
TKB	11	0.11	1.89	0.17	1.68
Total (single scan)	469	-0.85	2.48	-0.04	2.28
Total (station bias)	27	-0.82	1.24	0.11	1.11

1

2

(b)

3

4

Ocean	Differences between uncorrected GOSAT XCO ₂ and aircraft-based XCO ₂			Differences between corrected GOSAT XCO ₂ and aircraft-based XCO ₂		
	site	number	average [ppm]	SD [ppm]	average [ppm]	SD [ppm]
FCO	1	0.12	—	-3.39	—	
NRT	4	-4.27	3.24	-2.89	2.49	
HND	1	0.86	—	2.51	—	
NGO	3	-1.43	0.77	-0.02	0.58	
KIX	4	-3.00	1.95	-1.86	1.56	
HNL	19	-1.49	1.06	0.66	1.36	
BKK	2	-3.40	0.96	-1.10	0.24	
SIN	4	-2.33	1.70	0.06	2.05	
CGK	2	-2.46	3.12	0.57	0.25	
SYD	5	-1.52	1.28	-0.03	1.04	
NHA	3	-1.56	1.07	-1.60	2.06	
SCA	5	-2.67	2.05	-0.45	1.99	
TGC	2	-2.36	0.12	-0.52	0.02	



RTA	6	-2.93	1.75	-0.39	1.36
MNM	3	-1.39	0.61	-0.45	1.41
HPB	1	-0.16	—	0.86	—
HPD	1	-2.21	—	0.07	—
HPG	1	-3.29	—	-1.89	—
Total (single scan)	67	-2.08	1.69	-0.32	1.74
Total (station bias)	18	-1.97	1.31	-0.55	1.41

1
2
3
4
5
6
7
8
9
10
11
12
13
14
15
16
17
18



1 Table 7. The average and standard deviation of the differences between uncorrected/corrected
 2 GOSAT XCH₄ and aircraft-based XCH₄ at each aircraft observation site. The GOSAT data
 3 were retrieved over (a) land and (b) ocean regions within ±5° latitude/longitude boxes
 4 centered at each site. The averages and standard deviations of the differences of the matched
 5 data at all aircraft observation sites (single scan) and those of the station biases are also shown
 6 in the second row from the bottom and the bottom row of the table, respectively.

7

Land		Differences between uncorrected GOSAT XCH ₄ and aircraft-based XCH ₄		Differences between corrected GOSAT XCH ₄ and aircraft-based XCH ₄	
site	number	average [ppb]	SD [ppb]	average [ppb]	SD [ppb]
DND	12	7.3	10.0	5.0	10.0
LEF	33	9.3	19.9	7.1	19.8
NHA	26	7.4	14.6	5.2	14.4
WBI	19	5.3	12.7	2.7	13.2
THD	4	-15.6	20.3	-17.9	20.6
BNE	5	9.4	9.1	7.0	9.0
CAR	44	5.6	13.7	3.2	14.1
HIL	32	2.6	14.3	0.1	14.2
AAO	21	0.6	15.4	-2.1	15.3
SCA	20	7.9	12.4	5.9	12.4
TGC	13	8.7	16.2	6.7	16.4
SGP	69	0.4	15.7	-1.8	15.8
YAK	8	3.0	17.6	0.4	17.5
SGM	7	2.7	9.4	-0.3	9.3
HPA	1	-10.6	—	-12.5	—
HPI	1	3.0	—	1.5	—
TKB	11	10.8	12.4	8.5	12.0
Total (single scan)	326	4.5	15.2	2.2	15.3
Total (station bias)	17	3.4	7.0	1.1	7.0

8



1

(b)

Ocean		Differences between uncorrected GOSAT XCH ₄ and aircraft-based XCH ₄		Differences between corrected GOSAT XCH ₄ and aircraft-based XCH ₄	
site	number	average [ppb]	SD [ppb]	average [ppb]	SD [ppb]
NHA	3	24.2	10.9	16.7	10.1
SCA	5	-4.9	9.1	-13.6	9.6
TGC	2	9.5	2.3	3.1	2.8
RTA	7	5.2	14.5	-3.0	15.2
MNM	4	13.1	8.2	3.6	8.0
HPC	1	-2.2	—	-7.9	—
HPE	1	7.5	—	1.4	—
HPF	1	4.9	—	-3.5	—
HPG	1	-0.2	—	-13.8	—
Total (single scan)	25	6.6	12.8	-1.7	13.3
Total (station bias)	9	6.4	8.8	-1.9	9.6

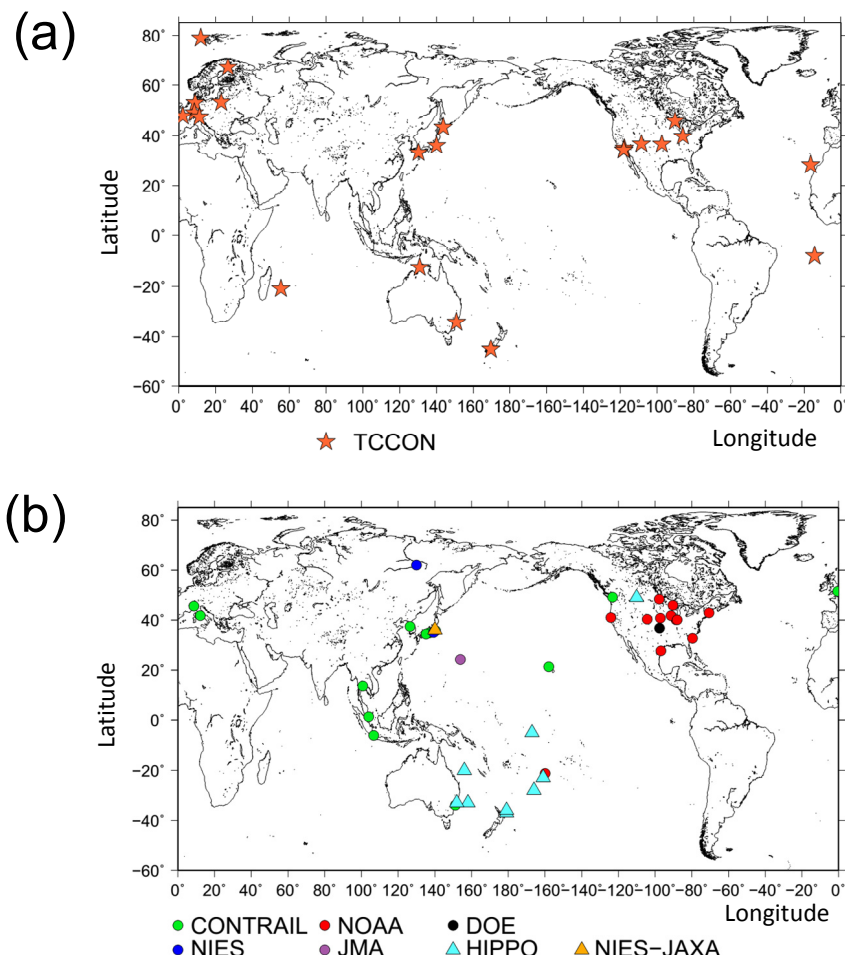
3

4

5



1



2

3

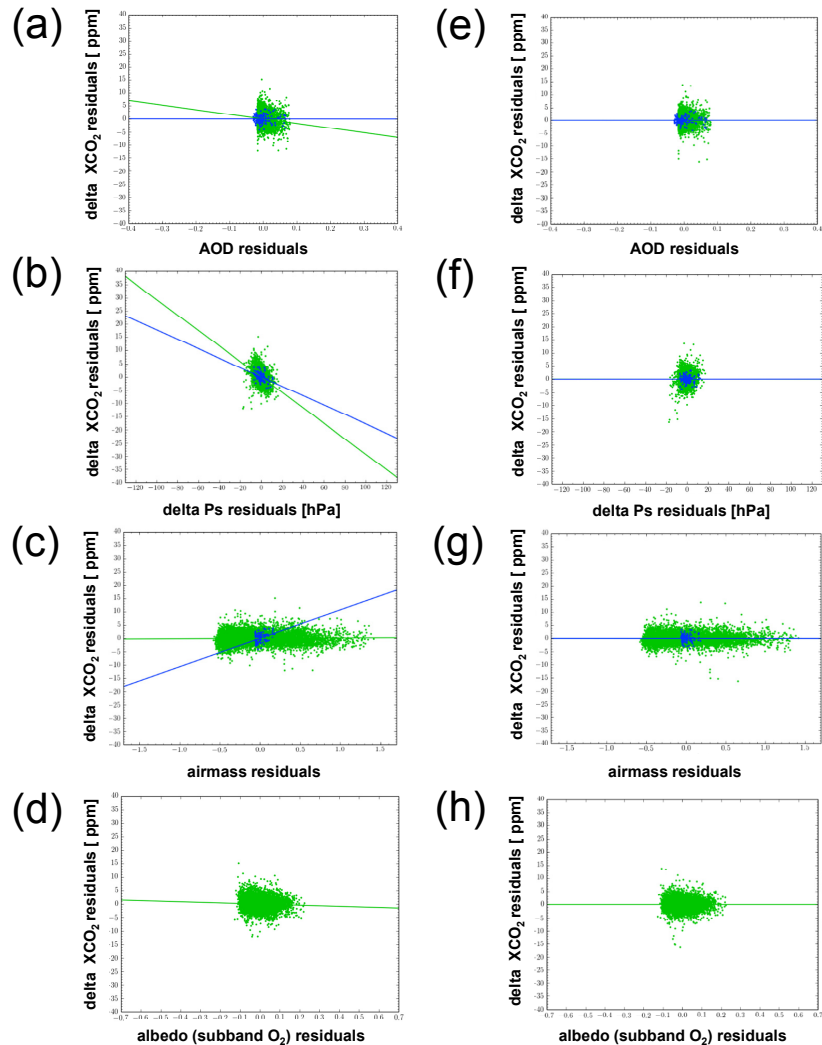
4

5 Fig. 1. Global distributions of (a) the TCCON sites used for correction and validation of
6 GOSAT data and (b) the aircraft observation sites used for validation of GOSAT data.

7

8

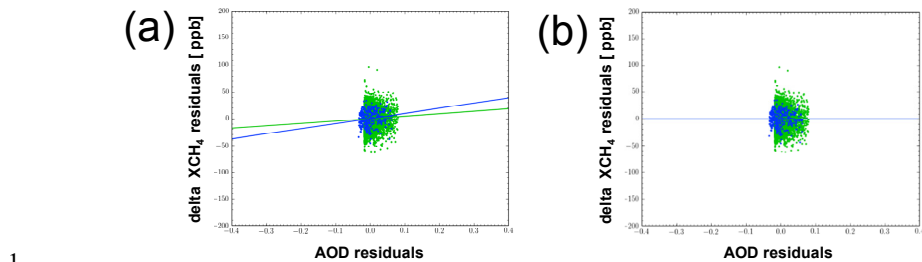
9



1

2 Fig. 2. Scatter diagrams between ΔXCO_2 calculated from uncorrected GOSAT data and (a)
 3 the retrieved aerosol optical depth, (b) the difference between the retrieved and a priori
 4 surface pressures, (c) airmass, and (d) surface albedo for the O₂ A-band. Scatter diagrams
 5 between ΔXCO_2 calculated from corrected GOSAT data and (e) the retrieved aerosol optical
 6 depth, (f) the difference between the retrieved and a priori surface pressures, (g) airmass, and
 7 (h) surface albedo for the O₂ A-band. Green (blue) dots and lines indicate the GOSAT data
 8 and regression lines over land (ocean) regions.

9



1

2

3 Fig. 3. Scatter diagrams between ΔXCH_4 calculated from (a) uncorrected and (b) corrected
4 GOSAT data and the retrieved aerosol optical depth. Green (blue) dots and lines indicate the
5 GOSAT data and the regression lines over land (ocean) regions.

6

7

8

9

10

11

12

13

14

15

16

17

18

19

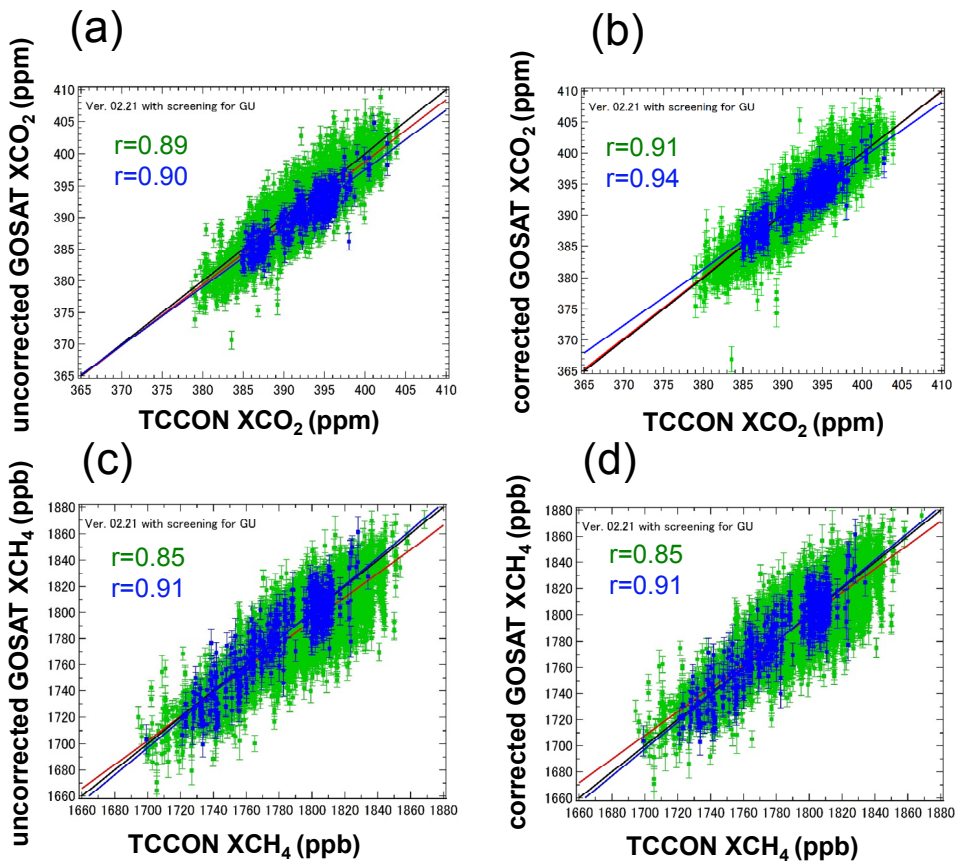
20

21



1

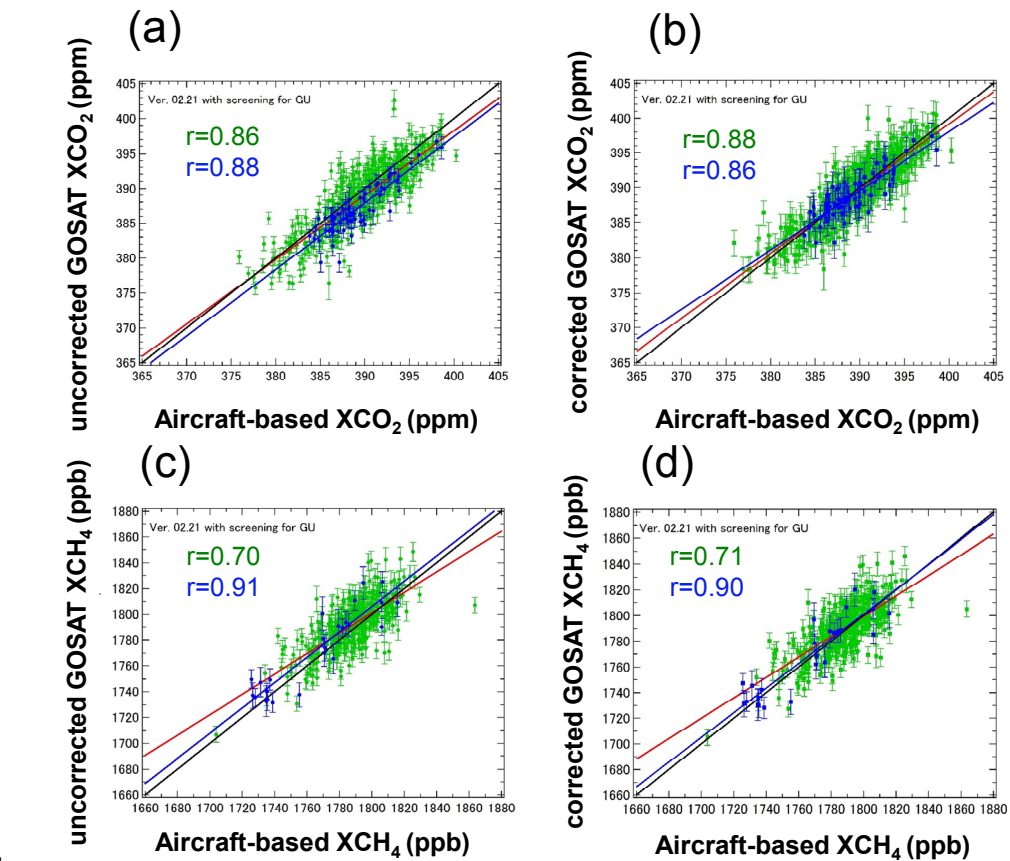
2



3

4

5 Fig. 4. Scatter diagrams between (a) uncorrected and (b) corrected GOSAT XCO₂ observed
 6 within $\pm 5^\circ$ latitude/longitude boxes (centered at each TCCON site) and TCCON XCO₂
 7 measured on the same day. (c), (d), same as (a) and (b) for XCH₄. Green and blue dots
 8 indicate GOSAT data obtained over land and ocean regions, respectively. Red and blue lines
 9 denote the regression lines, statistically significant at the 99% level, over land and ocean
 10 regions, respectively. Black lines show the one-to-one correspondence.

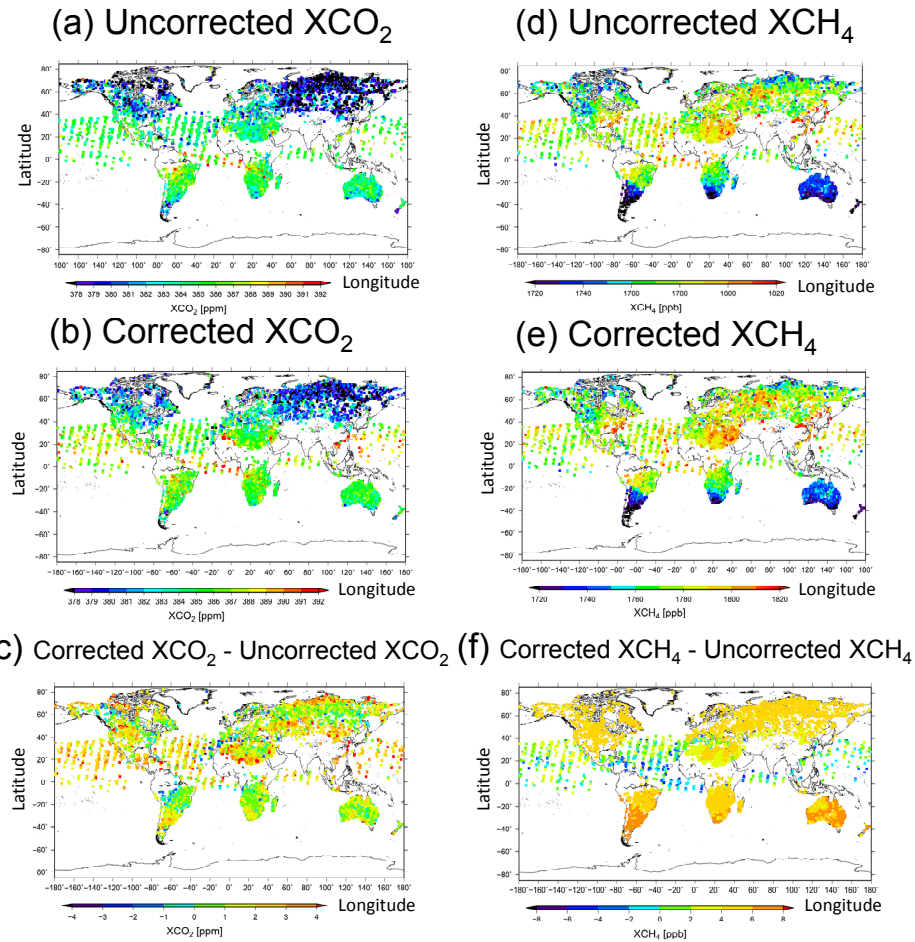


1

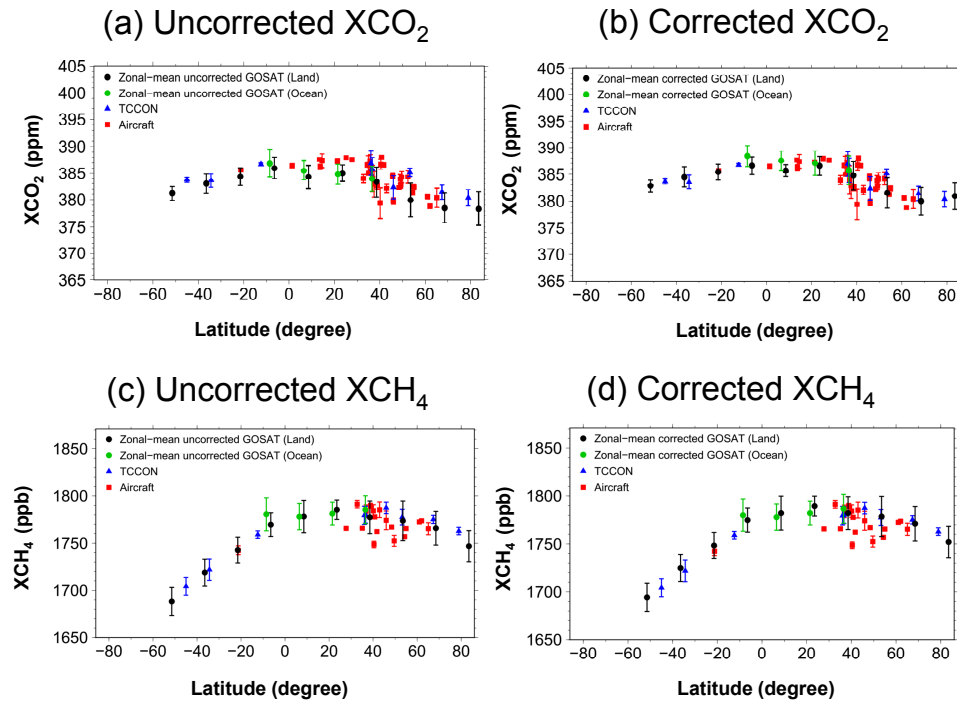
2

3 Fig. 5. Scatter diagrams between (a) uncorrected and (b) corrected GOSAT XCO₂ observed
 4 within $\pm 5^\circ$ latitude/longitude boxes (centered on each aircraft profile) and aircraft-based
 5 XCO₂ observed on the same day. (c), (d), same as (a) and (b) for XCH₄. Green and blue dots
 6 indicate the GOSAT data obtained over land and ocean regions, respectively. Red and blue
 7 lines denote the regression lines, statistically significant at the 99% level, over land and ocean
 8 regions, respectively. Black lines show the one-to-one correspondence.

9



1
2
3
4 Fig. 6. Global maps of (a) uncorrected and (b) corrected GOSAT XCO₂, and (d) uncorrected
5 and (e) corrected GOSAT XCH₄ in July 2009. The differences between corrected and
6 uncorrected (c) GOSAT XCO₂ and (f) GOSAT XCH₄.
7
8
9
10



1
 2
 3
 4 Fig. 7. Latitudinal distributions of (a) uncorrected and (b) corrected GOSAT XCO₂, TCCON
 5 XCO₂, and aircraft-based XCO₂ in July 2009. Latitudinal distributions of (c) uncorrected and
 6 (d) corrected GOSAT XCH₄, TCCON XCH₄, and aircraft-based XCH₄ in July 2009. Black
 7 and green circles indicate the zonal-mean GOSAT data retrieved over land and ocean regions,
 8 respectively. The blue triangles and red squares denote the TCCON data and aircraft-based
 9 data, respectively, at each observation site. See text for details.

10
 11
 12
 13
 14

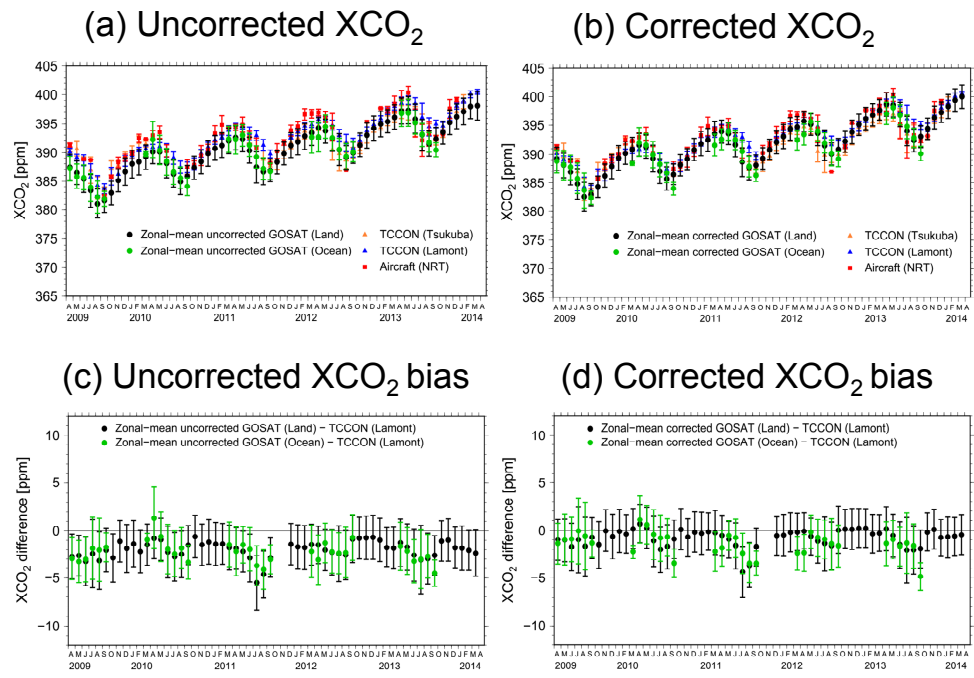


Fig. 8. Temporal variations of (a) uncorrected and (b) corrected GOSAT XCO_2 , TCCON XCO_2 , and aircraft-based XCO_2 . Black and green circles in (a) and (b) indicate the monthly zonal-mean GOSAT data retrieved over land and ocean regions, respectively, within a 30° – 45°N latitudinal band. The orange triangles, blue triangles, and red squares in (a) and (b) denote the TCCON XCO_2 at Tsukuba and Lamont, and aircraft-based XCO_2 at Narita, respectively. Temporal variations of the differences between (c) uncorrected and (d) corrected GOSAT XCO_2 and TCCON XCO_2 at Lamont ($\text{GOSAT } \text{XCO}_2$ minus $\text{TCCON } \text{XCO}_2$) over land (black dots) and ocean (green dots). See text for details.

12

13

14

15

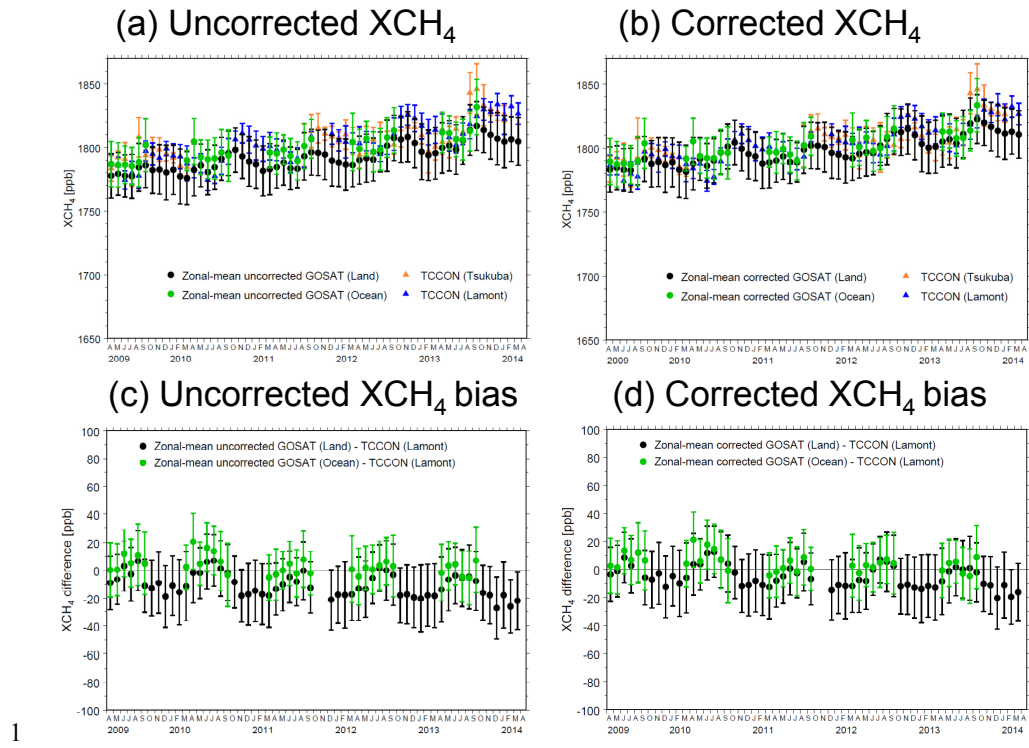


Fig. 9. Temporal variations of (a) uncorrected and (b) corrected GOSAT XCH₄ and TCCON XCH₄. Black and green circles in (a) and (b) indicate the monthly zonal-mean GOSAT data retrieved over land and ocean regions within a 30°–45°N latitudinal band, respectively. The orange and blue triangles in (a) and (b) denote the TCCON XCH₄ at Tsukuba and Lamont, respectively. Temporal variations of the differences between (c) uncorrected and (d) corrected GOSAT XCH₄ and TCCON XCH₄ at Lamont (GOSAT XCH₄ minus TCCON XCH₄) over land (black dots) and ocean (green dots). See text for details.